

①

学 位 論 文

Hadron-Hadron Interaction in Two-Dimensional World

(二次元時空でのハドロン-ハドロン相互作用)

平成4年12月博士(理学) 申請

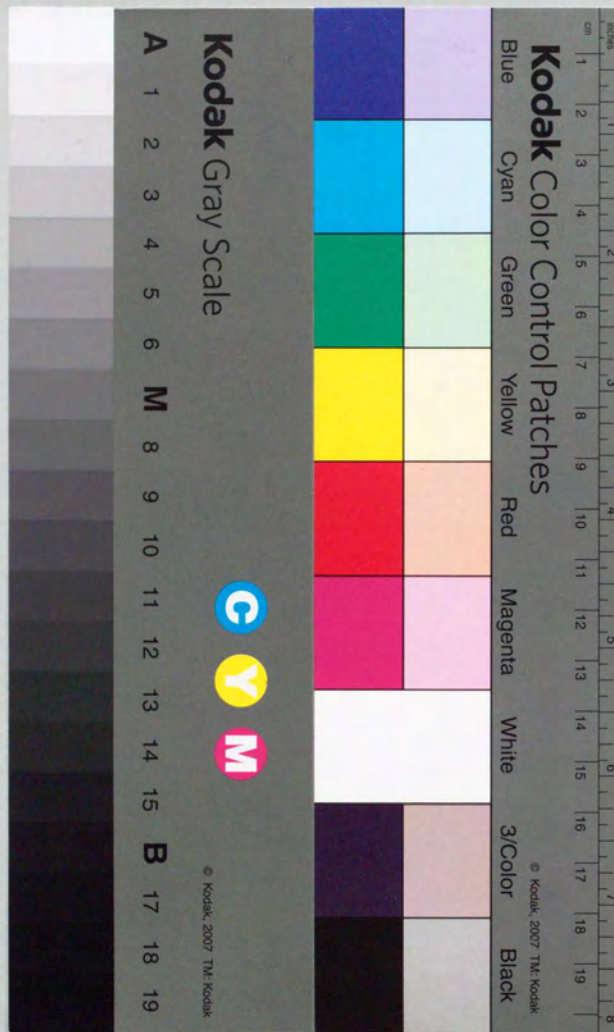
東京大学大学院理学系研究科

物理学専攻

蔵 本 武 志

UNIVERSITY OF TOKYO

December 1992





①

学 位 論 文

Hadron-Hadron Interaction in Two-Dimensional World

(二次元時空でのハドロン-ハドロン相互作用)

平成4年12月博士(理学) 申請

東京大学大学院理学系研究科

物理学専攻

蔵 本 武 志

**Hadron-Hadron Interaction in Two-Dimensional World**

by

**Takeshi Kuramoto**

Submitted to the Department of Physics

in Partial Fulfillment of

the Requirements for the Degree of

DOCTOR OF PHILOSOPHY

at the

UNIVERSITY OF TOKYO

December 1992



## Contents

<b>1</b>	<b>Introduction</b>	<b>2</b>
<b>2</b>	<b>Hadron States</b>	<b>7</b>
2.1	Formulation . . . . .	7
2.2	Results and Discussion . . . . .	15
<b>3</b>	<b>Interaction between Heavy Mesons</b>	<b>18</b>
3.1	Quark Exchange Potential . . . . .	19
3.2	Meson Exchange Potential . . . . .	27
<b>4</b>	<b>Summary and Conclusion</b>	<b>31</b>



## 1 Introduction

Quantum chromodynamics (QCD) is now believed to be the theory of strong interactions, that is to say, to describe the hadron physics. Hadrons are composite particles of quarks and gluons. QCD describes the interactions between quarks and gluons. Short distance behavior of QCD is known as asymptotic freedom [1] and has been extensively studied by the perturbation theory, e.g. the quark-parton model [2] which is rigorously derived from the short distance behavior. Many people have tried to understand its long distance behavior, i.e. the mechanism of confinement, the hadron spectra and the hadron-hadron interactions but there has been no satisfactory explanation of them apart from numerical simulations based on the lattice gauge theory.

We can not observe the original interactions between quarks and gluons directly because of the confinement. We can only observe hadrons and their interactions. We are therefore interested in the connection between the hadron spectra and the original interactions and that between hadron-hadron interactions and the original ones. These connections have been studied via the constituent quark model [3,4] for example. This model has been partially successful in describing hadron spectra [3] and hadron-hadron interactions [4] in the real world. The quark cluster model is an example of the model. The model assumes that a hadron consists of quarks moving nonrelativistically and interacting with each other through the confining potential and some other residual interaction such as the perturbative one-gluon exchange potential. Therefore, the model is missing the important properties, that is to say the Lorentz covariance and the chiral symmetry.

One of the difficulties in four dimensional QCD is caused by the existence of active

gluons. It is known that, by reducing the number of the space-time dimensions, there are no active gluons in two dimensional QCD (QCD<sub>2</sub>) [5]. In QCD<sub>2</sub>, we can find in the axial gauge a Hamiltonian which is a sum of the Dirac Hamiltonian for quarks and the instantaneous color Coulomb interaction between the quarks without any approximations. Though the appearance of the instantaneous interaction seems to contradict with the Lorentz covariance, it is an artifact of choosing a particular gauge and the resulting hadron systems are certainly covariant. These are important features that are missing in the quark cluster model. In two dimensions the confinement is trivial, and therefore we can not expect to understand the mechanism of confinement in four dimensional QCD. The spontaneous chiral symmetry breaking is another important aspect of QCD in four dimensions [6] but, according to Coleman's theorem [7], the spontaneous symmetry breaking does not take place in two dimensions. We will here deal with QCD<sub>2</sub> at the mean field level. At this level, Coleman's theorem is not applicable and there is the spontaneous symmetry breaking [8,9,10]. In fact the ground state meson is massless in the case of massless quark and is considered to be the Goldstone boson [11]. For QCD<sub>2</sub>, analytical or semi-analytical treatments are available and it has still some features in common with QCD in four dimensions. QCD<sub>2</sub> gives rise to hadron spectra corresponding to the string structure of hadrons which explains the observed Regge trajectories of hadrons in four dimensions [12]. The calculated form factors [13] of the two dimensional hadrons are also similar to the observed ones in the real world. Both of their asymptotic behaviors are characterized by  $1/q^2$ . Moreover, in two dimensions, we can see the relation between QCD and the naive parton model even in the processes where long distance effects play an important role [13,14]. We therefore expect that we can learn something about the hadron-hadron interactions in four dimensional QCD by



studying in  $\text{QCD}_2$  [14]-[17].

$\text{QCD}_2$  has been studied by many theorists since the pioneering work of 't Hooft [12]. Using the light-cone formulation he showed that, in the limit of large number of colors, the hadronic world in two dimensions consists of non-interacting mesons and the meson spectra is given by solving a simple one-variable integral equation called the 't Hooft equation. (We note that although the theory is solvable only in the large  $N$  (number of colors) limit, basic features of hadron spectra seem to remain the same for finite  $N$  [11].) The interaction between the mesons, which is of order  $1/N$ , has also been studied in the light-cone formulation [15,16,17]. Although we can in principle learn from these studies the general features of hadronic interactions in the two dimensional world, the use of the light-cone formulation discourages us from expressing them in more intuitive ways, such as in the form of potentials between hadrons, and at least no one has ever tried this. The interactions can be expressed in terms of potentials in the ordinary coordinate formulation [5] but the single meson problem becomes appreciably involved as we will see later and the calculation of the meson-meson interaction for general cases seems too complicated to allow us analytical insights.

In this thesis, we choose the case which is sufficiently interesting but is simple enough to allow us analytical or semi-analytical understanding. For this purpose, we consider a heavy meson consisting of a light quark and a heavy antiquark and calculate the interaction between two such mesons in the large  $N$  limit. We will show that, in such a case, the only role of light antiquarks is to give rise to the light meson exchange potential. The remaining potential can be described within the framework of the ordinary quantum mechanics without light antiquarks, that is to say the exchange of light quarks. After all, in  $\text{QCD}_2$  in the large  $N$  limit, the quark exchange and the meson exchange

contributions are unified in a natural way. This is the decisive difference between  $\text{QCD}_2$  and the hybrid model based on the quark cluster model [18,19] in which the quark exchange and the meson exchange are combined artificially to explain the hadron-hadron interaction in the real world.  $\text{QCD}_2$  therefore gives us a concrete example of examining the hybrid model in the real world where its theoretical basis has not been established so far.

We discuss the single meson states in Sec. 2. In Sec. 2.1 we will review the ordinary coordinate formulation with the axial gauge used by Bars and Green [5] and the 't Hooft equation as the result of going to the infinite momentum limit. In Sec. 2.2 we will present the meson spectra and the heavy meson ground state wave functions by the numerical calculation. We will discuss the equivalence between heavy meson states in the light-cone formulation and those in the usual coordinate formulation because in this case the equivalence is not self-evident. We will also make a comparison of spectra in the above two formulations for the light meson to examine the accuracy of the Tamm-Dancoff approximation in the ordinary coordinate formulation. Moreover we will present the meson energy spectra for finite momentum to examine their Lorentz invariance.

We will then calculate the interaction energy between the two heavy mesons as a function of their spatial separations in Sec. 3. The quark exchange potential is discussed in Sec. 3.1. In Sec. 3.2, we calculate the meson exchange potential. We restrict ourselves to the cases where the light meson is well described by  $q\bar{q}$  configurations only, i.e. in the Tamm-Dancoff approximation. Although the final results are obtained by numerical calculations, we try to understand the qualitative features in an analytical way as much as possible. We will examine the similarity in their potentials for two and



four dimensions.

In Sec. 4, we will summarize the results of our calculation and give concluding remarks.

## 2 Hadron States

### 2.1 Formulation

The purpose of this thesis is to discuss the hadron-hadron interaction in QCD<sub>2</sub>. First we will study single hadron states and review two methods to construct them, i.e. the ordinary coordinate treatment in the axial gauge and the light-cone treatment. The latter was used by 't Hooft [12], while the former as well as the equivalence of the two have been discussed in more detail by Bars and Green [5]. We will repeat here those part of their treatments that are necessary for the construction of light and heavy mesons.

The theory is defined by the SU(N) locally gauge-invariant Lagrangian

$$\mathcal{L} = -\frac{1}{4}F_{\mu\nu}^a F^{a\mu\nu} + \bar{\psi}(\frac{1}{2}i\gamma^\mu \overleftrightarrow{D}_\mu - m)\psi, \quad (2.1.1)$$

where

$$F_{\mu\nu}^a = \partial_\mu A_\nu^a - \partial_\nu A_\mu^a + gf^{abc}A_\mu^b A_\nu^c, \quad (2.1.2)$$

$$D_\mu = \partial_\mu - igA_\mu^a \frac{\lambda^a}{2}. \quad (2.1.3)$$

Here the indices on the quark fields  $\psi$  corresponding to color  $i$  ( $i = 1, \dots, N$ ), flavor ( $A, B, \dots$ ) and Dirac spinor are suppressed. The gluon fields  $A_\mu^a$  have  $N^2 - 1$  color components ( $a = 1, \dots, N^2 - 1$ ). Following Ref. [5], we choose the  $\gamma$ -matrix convention in two dimensions as  $\gamma^0 = \sigma_3$ ,  $\gamma^1 = i\sigma_2$  and  $\gamma_5 = \gamma^0\gamma^1 = \sigma_1$ .  $\lambda^a$  is an SU(N) color generator matrix which is normalized such that

$$\text{Tr}(\lambda^a \lambda^b) = 2\delta^{ab}. \quad (2.1.4)$$

We use here the Hamiltonian in the usual coordinate based on the axial gauge, i.e.  $A_1^a = 0$  [5]. Using the constraints of the gauge fixing and the Lagrange equation of



motion, we can eliminate the gauge field in the Hamiltonian. We refer to Ref. [5] for the detailed derivation of the Hamiltonian in the color singlet sector which is given by

$$H = \int dx \psi^\dagger \left( -\frac{i}{2} \gamma_5 \vec{\partial}_1 + \gamma^0 m \right) \psi - \frac{1}{4} \int dx dy \rho^a(x, t) |x - y| \rho^a(y, t), \quad (2.1.5)$$

where  $\rho^a = \psi^\dagger g \frac{\lambda^a}{2} \psi$ .

The ground state of the Hamiltonian (the vacuum state) is known to be given by the Hartree-Fock approximation in the large  $N$  limit [10]. In fact we will show later that the contributions to the total energy from the diagrams beyond the Hartree-Fock approximation are higher order in  $1/N$ . We expand a quark field  $\psi(x)$  in terms of the momentum eigenstates

$$\psi_\alpha(x, t) = \int \frac{dk}{2\pi} [b^i(k, t) u_\alpha(k) e^{ikx} + d^{ti}(k, t) v_\alpha(k) e^{-ikx}], \quad (2.1.6)$$

where  $u(k)$  and  $v(k)$  are single particle wave functions to be specified later and  $b^i$  and  $d^{ti}$  are a destruction operator of a quark and a creation operator of an antiquark, respectively. We require single particle wave functions to have the following properties. Orthogonality:

$$u^\dagger(k) u(k) = v^\dagger(-k) v(-k) = 1, \quad (2.1.7)$$

$$u^\dagger(k) v(-k) = 0. \quad (2.1.8)$$

Completeness:

$$u_\alpha(k) u_\beta^\dagger(k) + v_\alpha(-k) v_\beta^\dagger(-k) = \delta_{\alpha\beta}. \quad (2.1.9)$$

With these properties and the usual anti-commutation relations for the quark fields, the canonical anti-commutation relations become

$$\{b^i(k, t), b^{tj}(k', t)\} = 2\pi \delta(k - k') \delta^{ij}, \quad (2.1.10)$$

$$\{d^i(k, t), d^{tj}(k', t)\} = 2\pi \delta(k - k') \delta^{ij}, \quad (2.1.11)$$

and all other anti-commutators are zero. We define the vacuum state as follows:

$$b^i|0\rangle = d^i|0\rangle = 0. \quad (2.1.12)$$

We will determine the single particle wave functions by minimizing the vacuum expectation value of the Hamiltonian [10]. The expectation value in the large  $N$  limit is

$$\langle 0 | H | 0 \rangle = N \int dx \int \frac{dp}{2\pi} [v^\dagger(-p)(p\gamma_5 + m\gamma^0)v(-p) - \frac{\xi}{2} P \int \frac{dk}{(p-k)^2} v^\dagger(-p)v(-k)v^\dagger(-k)v(-p)], \quad (2.1.13)$$

where

$$\xi \equiv \frac{g^2 N}{4\pi}, \quad (2.1.14)$$

and we have used Eq. (2.1.9) and the following relation derived from the normalization of the color generator Eq. (2.1.4):

$$\frac{\lambda_{ij}^a}{2} \frac{\lambda_{kl}^a}{2} = \frac{1}{2} (\delta_{il} \delta_{jk} - \frac{1}{N} \delta_{ij} \delta_{kl}). \quad (2.1.15)$$

$P$  stands for the principal value and therefore

$$P \int \frac{dk}{(p-k)^2} = 0, \quad (2.1.16)$$

which has been used in obtaining the expression (2.1.13). Using Lagrange's method of undetermined multipliers, we minimize  $\langle 0 | H | 0 \rangle$  under the condition that the single particle wave functions satisfy the orthogonality. We obtain an eigenvalue equation for the occupied negative energy wave function  $v(-p)$  by functional differentiation with respect to  $v^\dagger(-p)$ .

$$-E(p)v(-p) = [p\gamma_5 + m\gamma^0 - \xi P \int \frac{dk}{(p-k)^2} v(-k)v^\dagger(-k)]v(-p). \quad (2.1.17)$$



This equation is to be solved self-consistently. To do so, we give the explicit form of the single particle wave functions satisfying the orthogonality, Eqs. (2.1.7) and (2.1.8), and the completeness, Eq. (2.1.9). Its general forms are given by

$$u(k) = T(k) \begin{pmatrix} 1 \\ 0 \end{pmatrix}, \quad v(-k) = T(k) \begin{pmatrix} 0 \\ 1 \end{pmatrix}, \quad (2.1.18)$$

where  $T(k)$  is a  $2 \times 2$  unitary matrix in Dirac space. Let us derive the equation that is easier to solve than Eq. (2.1.17). At first we multiply  $v^\dagger(-p)$  from the right-hand side and write the above equation in a matrix form

$$\begin{aligned} & -E(p)T(p)(1 - \gamma_0)T^\dagger(p) \\ & = [p\gamma_3 + m\gamma^0 + \frac{\xi}{2}P \int \frac{dk}{(p-k)^2} T(k)\gamma^0 T^\dagger(k)]T(p)(1 - \gamma_0)T^\dagger(p). \end{aligned} \quad (2.1.19)$$

We take the single particle wave functions to be real that is sufficiently general for our considerations (cf. Ref. [5]). So as to be, we take for the unitary transformation

$$T(p) = \exp[-\frac{1}{2}\theta(p)\gamma^1]. \quad (2.1.20)$$

We find the following four equations

$$E(p) \cos \theta(p) = m + \frac{\xi}{2}P \int \frac{dk}{(p-k)^2} \cos \theta(k), \quad (2.1.21)$$

$$E(p) \sin \theta(p) = p + \frac{\xi}{2}P \int \frac{dk}{(p-k)^2} \sin \theta(k), \quad (2.1.22)$$

$$p \cos \theta(p) - m \sin \theta(p) = \frac{\xi}{2}P \int \frac{dk}{(p-k)^2} \sin[\theta(p) - \theta(k)], \quad (2.1.23)$$

$$E(p) = m \cos \theta(p) + p \sin \theta(p) + \frac{\xi}{2}P \int \frac{dk}{(p-k)^2} \cos[\theta(p) - \theta(k)]. \quad (2.1.24)$$

Among the above four, only two of them are independent and any two of them can be derived from the remaining two. We choose the last two decoupled equations to obtain the quark single particle wave functions and the quark single particle energy. Solving

the self-consistent equation for  $\theta$ , Eq. (2.1.23), we get the single particle wave functions. Substituting then the obtained  $\theta$  into Eq. (2.1.24), we obtain the single particle energy. The solutions are given in Ref. [20]. We have reproduced their results, which are shown in Figs. 1 and 2. We see in Fig. 2 that  $E(p)$  is not positive definite. This is not surprising since the single particle states are colored and therefore their energies,  $E(p)$ , calculated with the Hamiltonian, Eq. (2.1.5), which is applicable only to color-singlet states, are not real ones. In fact, the single particle states are introduced to define the vacuum but they are not observable states themselves. They are neither gauge invariant nor covariant.

Let us briefly consider going beyond the Hartree-Fock approximation to confirm that the Hartree-Fock energy is dominant in  $1/N$  expansion. Examples of the diagrams contributing to the total energy which are the next order in perturbation theory are shown in Figs. 3(a) and (b). We calculate the order in  $1/N$  of the contribution of Figs. 3. The contribution of Fig. 3(a) is proportional to

$$g \frac{\lambda_{ji}^b}{2} g \frac{\lambda_{ij}^a}{2} g \frac{\lambda_{ik}^b}{2} g \frac{\lambda_{ki}^a}{2} = \frac{1}{4} g^4 N^2 (1 - \frac{1}{N^2}). \quad (2.1.25)$$

This is of the order 1 and therefore is of the higher order in  $1/N$  compared with the vacuum expectation value of the Hamiltonian given in Eq. (2.1.13). The contribution of Fig. 3(b) is proportional to

$$g \frac{\lambda_{ii}^a}{2} g \frac{\lambda_{ik}^b}{2} g \frac{\lambda_{kj}^a}{2} g \frac{\lambda_{ji}^b}{2} = -\frac{1}{4} g^4 N (1 - \frac{1}{N^2}). \quad (2.1.26)$$

This is of the order  $1/N$  and therefore is even higher in the order of  $1/N$  compared with the previous contribution. Similar considerations on the color matrix elements tell us that the ground state of the Hamiltonian is given by the Hartree-Fock approximation in the large  $N$  limit as we referred before.



We list up the Feynman rules for the later use. The fermion propagator can be obtained by direct calculation,

$$\langle 0 | T[\psi_\alpha^i(x) \bar{\psi}_\beta^j(y)] | 0 \rangle = \int \frac{dp d^0 p}{(2\pi)^2} e^{-ip_\mu(x-y)^\mu} i\delta^{ij} S(p^\mu)_{\alpha\beta}, \quad (2.1.27)$$

with

$$S(p^\mu) = \frac{u(p)\bar{u}(p)}{p^0 - E(p) + i\epsilon} + \frac{v(-p)\bar{v}(-p)}{p^0 + E(p) - i\epsilon}. \quad (2.1.28)$$

The interaction in the present formulation is the instantaneous Coulomb potential given by the second term on the r.h.s. of Eq. (2.1.5), and its matrix elements can be calculated by combining the "gluon propagator"

$$-i \frac{P}{k^2} \delta_{ab}, \quad (2.1.29)$$

and the "quark-gluon vertex"

$$ig\gamma^0 \frac{\lambda_{ij}^a}{2}. \quad (2.1.30)$$

Now we are ready to derive the equation for mesons which are the color-singlet bound states of quark-antiquark pairs. 't Hooft showed that, in the large  $N$  limit, we have nothing but the ladder diagrams in which all "gauge field" lines must be between the fermion lines and may not cross each other [12]. Thus the equation for the meson wave function,  $\Psi(r^\mu, p^\mu)$ , is given by a Bethe-Salpeter equation, depicted in Fig. 4, whose interaction kernel consists of the lowest order term of the quark-antiquark Coulomb potential:

$$\Psi(r^\mu, p^\mu) = \frac{i\xi}{2\pi} P \int \frac{dk dk^0}{(p-k)^2} S^A(p^\mu) \gamma^0 \Psi(r^\mu, k^\mu) \gamma^0 S^B(p^\mu - r^\mu), \quad (2.1.31)$$

where  $r^\mu$  is the total momentum of the bound states and  $p^\mu$  is the momentum of the quark and  $A$  and  $B$  refer to the flavor. Writing

$$\phi(r, p) = \int \frac{dp^0}{2\pi} \Psi(r^\mu, p^\mu), \quad (2.1.32)$$

we have for  $\phi$

$$\phi(r, p) = \xi P \int \frac{dk}{(p-k)^2} \left[ \frac{u^A(p)\bar{u}^A(p)\gamma^0 \phi(r, k)\gamma^0 v^B(r-p)\bar{v}^B(r-p)}{E^A(p) + E^B(r-p) - r^0} + \frac{v^A(-p)\bar{v}^A(-p)\gamma^0 \phi(r, k)\gamma^0 u^B(p-r)\bar{u}^B(p-r)}{E^A(p) + E^B(r-p) + r^0} \right]. \quad (2.1.33)$$

Using Eq. (2.1.18), we obtain

$$\tilde{\phi}(r, p) = \xi P \int \frac{dk}{(p-k)^2} \left[ \frac{1 + \gamma^0}{2} \frac{T^A(p)T^A(k)\tilde{\phi}(r, k)T^{B\dagger}(r-k)T^B(r-p)}{E^A(p) + E^B(r-p) - r^0} \frac{1 - \gamma^0}{2} + \frac{1 - \gamma^0}{2} \frac{T^A(p)T^A(k)\tilde{\phi}(r, k)T^{B\dagger}(r-k)T^B(r-p)}{E^A(p) + E^B(r-p) + r^0} \frac{1 + \gamma^0}{2} \right], \quad (2.1.34)$$

where  $\tilde{\phi}$  is defined by  $\phi$  through two unitary transformations,  $T^A$  and  $T^B$ , i.e.

$$\tilde{\phi}(r, p) \equiv T^{A\dagger}(p)\phi(r, p)T^B(r-p). \quad (2.1.35)$$

From the structure of  $\tilde{\phi}$  in the Dirac space, as given by Eq. (2.1.34),  $\tilde{\phi}$  can be expressed as a linear combination of  $\gamma_5$  and  $\gamma^1$ . Therefore, we can write

$$\tilde{\phi} = \phi_+ M^+ + \phi_- M^-, \quad (2.1.36)$$

where the matrices  $M^\pm$  are defined by

$$M^\pm = \frac{1}{2}(1 \pm \gamma^0)\gamma_5. \quad (2.1.37)$$

Substituting Eq. (2.1.36) into Eq. (2.1.34), we find a coupled integral equation for the meson wave function

$$\begin{aligned} & [E^A(p) + E^B(r-p) - r^0]\phi_+(r, p) \\ &= \xi P \int \frac{dk}{(p-k)^2} [C(p, k, r)\phi_+(r, k) + S(p, k, r)\phi_-(r, k)], \end{aligned} \quad (2.1.38)$$

$$\begin{aligned} & [E^A(p) + E^B(r-p) + r^0]\phi_-(r, p) \\ &= \xi P \int \frac{dk}{(p-k)^2} [C(p, k, r)\phi_-(r, k) + S(p, k, r)\phi_+(r, k)], \end{aligned} \quad (2.1.39)$$



where

$$C(p, k, r) = \cos\left[\frac{1}{2}\{\theta^A(p) - \theta^A(k)\}\right] \cos\left[\frac{1}{2}\{\theta^B(r-p) - \theta^B(r-k)\}\right], \quad (2.1.40)$$

$$S(p, k, r) = -\sin\left[\frac{1}{2}\{\theta^A(p) - \theta^A(k)\}\right] \sin\left[\frac{1}{2}\{\theta^B(r-p) - \theta^B(r-k)\}\right]. \quad (2.1.41)$$

Let us rewrite  $C(p, k, r)$  and  $S(p, k, r)$  to consider their meaning as Bars and Green have done, i.e.

$$C(p, k, r) = u^{A\dagger}(p)u^A(k)v^{B\dagger}(r-p)v^B(r-k), \quad (2.1.42)$$

$$S(p, k, r) = -v^{A\dagger}(-p)u^A(k)u^{B\dagger}(p-r)v^B(r-k). \quad (2.1.43)$$

$C$  and  $S$  appear in the diagrams shown in Figs. 5(a) and (b), respectively. That is to say,  $C(p, k, r)$  is associated with particle-antiparticle scattering process while  $S(p, k, r)$  is associated with the creation or destruction of two particle-antiparticle pairs. These are of course the basic processes in constructing a meson as depicted in Fig. 5(c).

For the light meson, Bars and Green have shown that the well known 't Hooft equation which is originally obtained by the light-cone coordinates with the light-cone gauge formulation can be obtained by taking the limit  $r \rightarrow \infty$ , which corresponds to going to the infinite momentum frame

$$r^2\phi_+(x) = \left(\frac{m_A^2 - 2\xi}{x} + \frac{m_B^2 - 2\xi}{1-x}\right)\phi_+(x) - 2\xi P \int_0^1 \frac{dy}{(y-x)^2} \phi_+(y), \quad (2.1.44)$$

and

$$\phi_-(x) = 0, \quad (2.1.45)$$

where  $x = p/r$  and  $y = k/r$ .

## 2.2 Results and Discussion

We will discuss the interaction between two heavy mesons, each consisting of a finite mass quark and an infinite mass antiquark. The equation for the heavy meson wave function is given by considering the limit of  $m_B \rightarrow \infty$ . In this limit  $\theta^B = 0$ ,  $E^B = m_B$ . Therefore Eqs. (2.1.38) and (2.1.39) become

$$[E^A(p) - p^0]\phi_+(r, p) = \xi P \int \frac{dk}{(p-k)^2} \cos\left[\frac{1}{2}\{\theta^A(p) - \theta^A(k)\}\right]\phi_+(r, k), \quad (2.2.1)$$

and

$$\phi_-(r, p) = 0, \quad (2.2.2)$$

where  $p^0 = r^0 - m_B$  is the energy of a light quark bound by a heavy antiquark. For the heavy meson  $S(p, k, r) = 0$  as the result of the fact  $\theta^B = 0$ . This means that the backward-moving string structure shown in Fig. 5(c) does not arise. That is to say, we have only to use Tamm-Dancoff approximation as long as we treat the heavy meson. We will use this fact later in the calculation of the interaction. We also see in Eq. (2.2.1) that the equation for a heavy meson wave function is independent of  $r$  and therefore the wave function can be written as a product of a function of single variable  $\phi_+(p)$  and an arbitrary function of  $r$ . In Figs. 6 we show of the ground state wave function in coordinate representation which is the Fourier transformation of  $\phi_+(p)$  for two cases,  $\xi = 0.5m_A^2$  and  $\xi = 5m_A^2$ .

As mentioned in Sec. 2.1, for the light meson, the 't Hooft equation can be obtained by going to the infinite momentum frame. The original theory is certainly covariant and therefore the meson mass spectra should be independent of the momentum. (In fact we will see later in explicit calculation.) Thus the mass spectra for  $m_B \gg r$  should be identical with those for  $r \gg m_B$  with a fixed  $m_B$  but we cannot see the equivalence in



the form of equations (2.1.44) and (2.2.1) in the limit  $m_B \rightarrow \infty$ . We therefore compare the spectra of the heavy meson calculated by Eq. (2.1.44) and Eq. (2.2.1). The results are listed in table 1. We find that the heavy meson spectra are identical with each other in these different calculations. (We regard the small differences in the table as numerical errors involved in the calculation.) It implies that the gauge invariance of the meson spectrum also holds for the heavy mesons.

The 't Hooft equation is much easier to solve than the coupled integral equations given by Eqs. (2.1.38) and (2.1.39) with the single particle equations given by Eqs. (2.1.23) and (2.1.24). In calculating the meson exchange interaction, we will neglect the contributions from the  $q\bar{q}$  pair moving backward (just as depicted in Fig. 5(c)) for the exchanged light meson, which corresponds to using the Tamm-Dancoff approximation also for the light meson. (This approximation amounts to neglecting  $\phi_-$  in Eq. (2.1.38).)

$$[E^A(p) + E^A(r-p) - r^0]\phi_+(r, p) = \xi P \int \frac{dk}{(p-k)^2} \cos\left[\frac{1}{2}\{\theta^A(p) - \theta^A(k)\}\right] \cos\left[\frac{1}{2}\{\theta^A(r-p) - \theta^A(r-k)\}\right] \phi_+(r, k). \quad (2.2.3)$$

We will therefore use the 't Hooft equation to check the accuracy of the approximation by comparing the spectra calculated by two methods. The results are listed in table 2. This shows that the Tamm-Dancoff approximation is good enough to construct the light meson for  $\xi = 0.5m_A^2$  and  $\xi = 5m_A^2$ . In the case of a very large value for the ratio,  $\xi/m_A^2$ , we are close to the chiral limit and the Tamm-Dancoff approximation is not applicable to the light meson. Inclusion of the backward moving diagrams (the random phase approximation) for the light meson appreciably complicates the calculation of the potential. We will therefore restrict ourselves to not too large values of the ratio. We also list the energy spectra,  $r_n^0$ , for finite momentum,  $r$ , in table 3. We can see the

relation,  $(r_n^0)^2 - r^2 = m_n^2$ , which means the Lorentz invariance of the meson spectra.



### 3 Interaction between Heavy Mesons

We now consider the interaction between two heavy mesons. We calculate its potential as a function of their spatial separations. It is well known that, in the large  $N$  limit, the theory becomes that of free mesons and the interaction is of the order of  $1/N$  compared with relevant energy scales such as the light meson masses and the energy eigenvalues,  $p^0$ , for the heavy meson. We will restrict ourselves to the first order term in  $1/N$ .

Let us first discuss the role of light antiquarks in this problem. We have seen in Sec. 2.2 that the light antiquarks do not appear in the wave function for a heavy meson to the lowest order in  $1/N$  since it is described by the Tamm-Dancoff approximation. The Hamiltonian for the color singlet sector, given by Eq. (2.1.5), involves the interaction term which gives rise to light quark-antiquark pair excitations, resulting in light meson clouds surrounding the  $q\bar{Q}$  state for the heavy meson. The mixing amplitudes of such light meson clouds in the heavy meson is of the order of  $1/\sqrt{N}$  as can be derived from the general argument of Ref. [21] (the amplitude of a diagram with  $n$  meson external lines is proportional to  $N^{(2-n)/2}$  to the leading order, so a 3-point vertex of meson is of the order of  $1/\sqrt{N}$ ) and also be seen by the explicit calculation in Sec. 3.2. We therefore expect a light meson exchange interaction between two heavy mesons to the order  $1/N$ . In fact, this is the only contribution that involves light antiquarks in the present problem, and we will calculate it in Sec. 3.2.

The remaining contribution to the interaction can thus be discussed within the framework of the ordinary quantum mechanics without particle production. We will take this approach for the calculation of quark exchange contributions in Sec. 3.1.

#### 3.1 Quark Exchange Potential

Let us first consider a single heavy meson consisting of a light quark, 1, and a heavy antiquark,  $\bar{1}$ , in the ordinary quantum mechanics. The eigenvalue problem given by Eq. (2.2.1) for the heavy meson is equivalent to that of a system described by the following Hamiltonian.

$$H_{1\bar{1}} = K_1 + V_{1\bar{1}}, \quad (3.1.1)$$

where  $K_1$  is the kinetic energy for the light quark, 1, related to  $E^A(p)$  as

$$\langle p | K_1 | q \rangle = 2\pi\delta(p-q)E^A(p), \quad (3.1.2)$$

where  $|p\rangle = b^\dagger(p)|0\rangle$ . The interaction,  $V_{1\bar{1}}$ , can be expressed as

$$V_{1\bar{1}} = \frac{\lambda_1^a}{2} \frac{\lambda_{\bar{1}}^a}{2} \tilde{V}_{1\bar{1}}. \quad (3.1.3)$$

$\tilde{V}_{1\bar{1}}$  in the momentum representation for the quark, 1, is then given by

$$\begin{aligned} i \langle p | \tilde{V}_{1\bar{1}} | q \rangle &= \int dx_1 e^{-ipx_1} e^{iqx_1} \bar{u}^A(p) i g \gamma^0 u^A(q) \\ &\quad \times \int \frac{dk}{2\pi} e^{ik(x_1-x_1)} (-i) \frac{P}{k^2} \bar{v}^B \cdot (-i) g \gamma^0 v^B \\ &= -i g^2 \frac{P}{(p-q)^2} \cos\left[\frac{1}{2}\{\theta^A(p) - \theta^A(q)\}\right] e^{-i(p-q)x_1}, \end{aligned} \quad (3.1.4)$$

where

$$v^B = \lim_{m_B \rightarrow \infty} T^B \begin{pmatrix} 0 \\ 1 \end{pmatrix} = \begin{pmatrix} 0 \\ 1 \end{pmatrix}. \quad (3.1.5)$$

In fact one can see that the eigenvalue problem of  $H_{1\bar{1}}$ ,

$$H_{1\bar{1}}\phi(1, \bar{1}) = p^0\phi(1, \bar{1}), \quad (3.1.6)$$

for a color singlet state reduces to Eq. (2.2.1). We present this derivation briefly. A color singlet state,  $\phi(1, \bar{1})$ , is represented by its spatial and color parts:

$$\phi(1, \bar{1}) = \varphi(x_1 - x_{\bar{1}}) \frac{1}{\sqrt{N}} \sum_i |i(1), i(\bar{1})\rangle, \quad (3.1.7)$$



where  $\varphi(x)$  is the Fourier transformation of the heavy meson wave function,  $\phi_+(p)$ .

$$\varphi(x_1 - x_1) = \int \frac{dq}{2\pi} \langle x_1 - x_1 | q \rangle \phi_+(q), \quad (3.1.8)$$

Multiplying  $\frac{1}{\sqrt{N}} \sum_j \langle j(1), j(\bar{1}) | \langle p |$  from the left hand side of Eq. (3.1.6) and using the Eqs. (3.1.2), (3.1.3), (3.1.4) and

$$\langle j(1), j(\bar{1}) | \lambda_1^a \lambda_{\bar{1}}^a | i(1), i(\bar{1}) \rangle = \lambda_{ji}^a \lambda_{i\bar{j}}^a, \quad (3.1.9)$$

we reduce Eq. (3.1.6) to Eq. (2.2.1).

We now consider a system of two heavy mesons consisting of two light quarks, 1 and 2, and two heavy antiquarks,  $\bar{1}$  and  $\bar{2}$ . The Hamiltonian can be written as

$$H = K_1 + K_2 + V_{12} + V_{1\bar{1}} + V_{1\bar{2}} + V_{2\bar{1}} + V_{2\bar{2}} + V_{\bar{1}\bar{2}}, \quad (3.1.10)$$

where  $V_{12}$  is the interaction between the two light quarks and is given in the momentum representation as

$$V_{12} = \frac{\lambda_1^a \lambda_2^a}{2} \tilde{V}_{12}, \quad (3.1.11)$$

$$\begin{aligned} & i \langle p_1, p_2 | \tilde{V}_{12} | q_1, q_2 \rangle \\ &= 2\pi \delta(p_1 + p_2 - q_1 - q_2) \\ & \times \bar{u}^A(p_1) i g \gamma^0 u^A(q_1) (-i) \frac{P}{(p_1 - q_1)^2} \bar{u}^A(p_2) i g \gamma^0 u^A(q_2) \\ &= 2\pi \delta(p_1 + p_2 - q_1 - q_2) \\ & \times i g^2 \frac{P}{(p_1 - q_1)^2} \cos\left[\frac{1}{2} \{\theta^A(p_1) - \theta^A(q_1)\}\right] \cos\left[\frac{1}{2} \{\theta^A(p_2) - \theta^A(q_2)\}\right]. \end{aligned} \quad (3.1.12)$$

$V_{\bar{1}\bar{2}}$  is the interaction between the two heavy antiquarks and is given by

$$V_{\bar{1}\bar{2}} = \frac{\lambda_{\bar{1}}^a \lambda_{\bar{2}}^a}{2} \tilde{V}_{\bar{1}\bar{2}}, \quad (3.1.13)$$

$$\begin{aligned} i \tilde{V}_{\bar{1}\bar{2}} &= \bar{v}^B \cdot (-i) g \gamma^0 v^B \int \frac{dk}{2\pi} e^{ik(x_1 - x_2)} (-i) \frac{P}{k^2} \bar{v}^B \cdot (-i) g \gamma^0 v^B \\ &= (-i) g^2 \frac{1}{2} |x_1 - x_2|. \end{aligned} \quad (3.1.14)$$

Other terms on the r.h.s. of Eq. (3.1.10) can be guessed from Eqs. (3.1.2), (3.1.3) and (3.1.4) and need not be repeated here.

We place the two heavy antiquarks,  $\bar{1}$  and  $\bar{2}$ , at  $X/2$  and  $-X/2$ , respectively, i.e.  $x_{\bar{1}} = X/2$  and  $x_{\bar{2}} = -X/2$  and calculate the ground state energy of the two heavy meson system. From now on we take  $\varphi(x)$  to be the Fourier transformation of the heavy meson ground state wave function in momentum space,  $\phi(p)$ . To the lowest order in  $1/N$ , the energy is just twice the eigenvalue,  $p^0$ , of a heavy meson and the wave function is an anti-symmetrized product of the two mesons, i.e.

$$\Psi(1, 2 : \bar{1}, \bar{2}) = \phi(1, \bar{1}) \phi(2, \bar{2}) - \phi(1, \bar{2}) \phi(2, \bar{1}). \quad (3.1.15)$$

In calculating the normalization of the wave function, we encounter the following terms for the color parts of the overlaps, i.e.

$$\begin{aligned} & \phi^\dagger(2, \bar{2}) \phi^\dagger(1, \bar{1}) \phi(1, \bar{1}) \phi(2, \bar{2}), \quad \phi^\dagger(2, \bar{1}) \phi^\dagger(1, \bar{2}) \phi(1, \bar{2}) \phi(2, \bar{1}), \\ & \phi^\dagger(2, \bar{2}) \phi^\dagger(1, \bar{1}) \phi(1, \bar{2}) \phi(2, \bar{1}), \quad \phi^\dagger(2, \bar{1}) \phi^\dagger(1, \bar{2}) \phi(1, \bar{1}) \phi(2, \bar{2}). \end{aligned}$$

The first one is given by

$$\begin{aligned} & \phi^\dagger(2, \bar{2}) \phi^\dagger(1, \bar{1}) \phi(1, \bar{1}) \phi(2, \bar{2}) \\ &= \varphi^2(x_1 - x_1) \varphi^2(x_2 - x_2) \frac{1}{N^2} \sum_{i, j, i', j'} \langle j'(2), j'(\bar{2}) | \langle i'(1), i'(\bar{1}) | i(1), i(\bar{1}) \rangle | j(2), j(\bar{2}) \rangle \\ &= \varphi^2(x_1 - x_1) \varphi^2(x_2 - x_2), \end{aligned} \quad (3.1.16)$$

and similarly, the second is  $\phi^\dagger(2, \bar{1}) \phi^\dagger(1, \bar{2}) \phi(1, \bar{2}) \phi(2, \bar{1}) = \varphi^2(x_2 - x_1) \varphi^2(x_1 - x_2)$ . The third one is given by



$$\begin{aligned}
& \phi^\dagger(2, \bar{2}) \phi^\dagger(1, \bar{1}) \phi(1, \bar{2}) \phi(2, \bar{1}) \\
&= \varphi(x_2 - x_2) \varphi(x_1 - x_1) \varphi(x_1 - x_2) \varphi(x_2 - x_1) \\
&\quad \times \frac{1}{N^2} \sum_{i,j,i',j'} \langle j'(2), j'(\bar{2}) | \langle i'(1), i'(\bar{1}) | i(1), i(\bar{2}) \rangle | j(2), j(\bar{1}) \rangle \\
&= \frac{1}{N} \varphi(x_2 - x_2) \varphi(x_1 - x_1) \varphi(x_1 - x_2) \varphi(x_2 - x_1), \quad (3.1.17)
\end{aligned}$$

and similarly, the fourth is

$\phi^\dagger(2, \bar{1}) \phi^\dagger(1, \bar{2}) \phi(1, \bar{1}) \phi(2, \bar{2}) = 1/N \varphi(x_2 - x_1) \varphi(x_1 - x_2) \varphi(x_1 - x_1) \varphi(x_2 - x_2)$ . Thus we obtain the normalization,

$$\begin{aligned}
\langle \Psi | \Psi \rangle &= 2 \int dx_1 dx_2 [\varphi^2(x_1 - X/2) \varphi^2(x_2 + X/2) \\
&\quad - \frac{1}{N} \varphi(x_1 - X/2) \varphi(x_1 + X/2) \varphi(x_2 + X/2) \varphi(x_2 - X/2)]. \quad (3.1.18)
\end{aligned}$$

We drop the second term in restricting ourselves to the leading order of  $1/N$ . One can use the first order perturbation theory to calculate the energy of the system to order  $1/N$ . The energy is thus given by the expectation value of the Hamiltonian,  $\langle \Psi | H | \Psi \rangle$ . Let us calculate this value. We use Eq. (3.1.6) to obtain

$$\begin{aligned}
H \Psi(1, 2 : \bar{1}, \bar{2}) &= (2p^0 + V_{12} + V_{1\bar{1}} + V_{2\bar{1}} + V_{1\bar{2}}) \phi(1, \bar{1}) \phi(2, \bar{2}) \\
&\quad - (2p^0 + V_{12} + V_{1\bar{1}} + V_{2\bar{2}} + V_{1\bar{2}}) \phi(1, \bar{2}) \phi(2, \bar{1}). \quad (3.1.19)
\end{aligned}$$

In calculating the color part of the matrix element  $\Psi^\dagger(1, 2 : \bar{1}, \bar{2}) H \Psi(1, 2 : \bar{1}, \bar{2})$ , we encounter the following types of the terms,

$$\begin{aligned}
\phi^\dagger(1, \bar{1}) V_{12} \phi(1, \bar{1}) &= \varphi(x_1 - x_1) \frac{1}{N} \sum_{i,j} \langle i(1), i(\bar{1}) | \frac{\lambda_1^a}{2} \frac{\lambda_2^a}{2} \bar{V}_{12} | j(1), j(\bar{1}) \rangle \varphi(x_1 - x_1) \\
&\propto \sum_{ij} \lambda_{ij} \delta_{ij} = 0, \quad (3.1.20)
\end{aligned}$$

which is the example of the direct term and

$$\begin{aligned}
& \phi^\dagger(2, \bar{2}) \phi^\dagger(1, \bar{1}) V_{12} \phi(1, \bar{2}) \phi(2, \bar{1}) \\
&= \varphi(x_2 - x_2) \varphi(x_1 - x_1) \bar{V}_{12} \varphi(x_1 - x_2) \varphi(x_2 - x_1) \\
&\quad \times \frac{1}{N^2} \sum_{i,j,i',j'} \langle i(2), i(\bar{2}) | \langle j(1), j(\bar{1}) | \frac{\lambda_1^a}{2} \frac{\lambda_2^a}{2} | i'(1), i'(\bar{2}) \rangle | j'(2), j'(\bar{1}) \rangle \\
&= \frac{1}{2} \varphi(x_2 - x_2) \varphi(x_1 - x_1) \bar{V}_{12} \varphi(x_1 - x_2) \varphi(x_2 - x_1), \quad (3.1.21)
\end{aligned}$$

which is the example of the exchange term. Thus we obtain

$$\begin{aligned}
\langle \Psi | H | \Psi \rangle &= 2p^0 \langle \Psi | \Psi \rangle \\
&\quad - \int dx_1 dx_2 \varphi(x_2 + X/2) \varphi(x_1 - X/2) [2\bar{V}_{1\bar{1}} + \bar{V}_{12} + \bar{V}_{1\bar{2}}] \\
&\quad \times \varphi(x_1 + X/2) \varphi(x_2 - X/2). \quad (3.1.22)
\end{aligned}$$

The quark exchange potential is then given by

$$V(X) \equiv \frac{\langle \Psi | H | \Psi \rangle}{\langle \Psi | \Psi \rangle} - 2p^0. \quad (3.1.23)$$

There are three types of interactions contributing to the potential, i.e. the interaction between a light quark and a heavy antiquark,  $V_{1\bar{1}}$  for example, that between light quarks,  $V_{12}$ , and that between heavy antiquarks,  $V_{1\bar{2}}$  as depicted in Figs. 7. We therefore decompose the potential into the corresponding three terms:

$$V(X) \equiv V_{qQ}(X) + V_{qq}(X) + V_{\bar{Q}\bar{Q}}(X). \quad (3.1.24)$$

Each terms are expressed in the momentum representation as follows:

$$\begin{aligned}
V_{qQ}(X) &= -2 \int dx_1 dx_2 \int \frac{dp}{2\pi} \langle p | x_1 - x_1 \rangle \phi(p) \bar{V}_{1\bar{1}} \int \frac{dq}{2\pi} \langle x_1 - x_2 | q \rangle \phi(q) \\
&\quad \times \int \frac{dk}{2\pi} e^{-ik(x_2 - x_1)} \phi(k) \int \frac{dk'}{2\pi} e^{ik'(x_2 - x_1)} \phi(k') / \langle \Psi | \Psi \rangle \\
&= -2 \int \frac{dp dq}{(2\pi)^2} \cos(qX) \phi(p) \phi(q) \langle p | \bar{V}_{1\bar{1}} | q \rangle |_{x_1=0} \\
&\quad \times \int \frac{dk}{2\pi} \phi^2(k) \cos(kX) / \langle \Psi | \Psi \rangle. \quad (3.1.25)
\end{aligned}$$



Similarly,

$$V_{qq}(X) = - \int \frac{dp_1 dp_2 dq_1 dq_2}{(2\pi)^4} \cos[(p_1 - q_2)X] \phi(p_1) \phi(p_2) \phi(q_1) \phi(q_2) \\ \times \langle p_1, p_2 | \tilde{V}_{12} | q_1, q_2 \rangle / \langle \Psi | \Psi \rangle, \quad (3.1.26)$$

$$V_{QQ}(X) = g^2 \frac{1}{2} |X| \left[ \int \frac{dk}{2\pi} \phi^2(k) \cos(kX) \right]^2 / \langle \Psi | \Psi \rangle, \quad (3.1.27)$$

where

$$\langle \Psi | \Psi \rangle = 2 \left\{ \int \frac{dp}{2\pi} \phi^2(p) \right\}^2, \quad (3.1.28)$$

which is normalized to 1.

We can see analytically the qualitative feature of the quark exchange potentials given by Eqs. (3.1.25), (3.1.26) and (3.1.27).  $V_{QQ}(X)$  is a product of the linear potential and the overlap of the wave functions,  $\varphi$ . Therefore, its behavior is easily foreseen, i.e. linearly rising near the origin, reaching maximum around the spatial extension of the heavy meson and decreasing rapidly as the overlap between the two heavy mesons gets poorer. Let us consider the remaining potentials,  $V_{qQ}(X)$  and  $V_{qq}(X)$ . To do so, we discuss at first their short distance behaviors.

$$V_{qQ}(0) = \sqrt{2} g^2 \int \frac{dp dq}{(2\pi)^2} \phi(p) \phi(q) \frac{P}{(p - q)^2} \cos\left[\frac{1}{2}\{\theta^A(p) - \theta^A(q)\}\right]. \quad (3.1.29)$$

This expression can be shown to be negative in following way. We define the Fourier transforms of  $\phi(p) \cos[\frac{1}{2}\theta^A(p)]$  and  $\phi(p) \sin[\frac{1}{2}\theta^A(p)]$  as  $\bar{\varphi}_c(x)$  and  $\bar{\varphi}_s(x)$ , respectively, i.e.

$$\bar{\varphi}_c(x) = \int \frac{dp}{2\pi} e^{ipx} \phi(p) \cos\left[\frac{1}{2}\theta^A(p)\right], \quad (3.1.30)$$

$$\bar{\varphi}_s(x) = \int \frac{dp}{2\pi} e^{ipx} \phi(p) \sin\left[\frac{1}{2}\theta^A(p)\right]. \quad (3.1.31)$$

The expression (3.1.29) can then be written as

$$V_{qQ}(0) = -\frac{g^2}{\sqrt{2}} \int dx [|\bar{\varphi}_c(x)|^2 + |\bar{\varphi}_s(x)|^2] |x|, \quad (3.1.32)$$

which is obviously negative. Thus

$$V_{qQ}(0) < 0. \quad (3.1.33)$$

A similar argument is also applicable to  $V_{qq}(0)$ .

$$V_{qq}(0) = -g^2 \int \frac{dp_1 dp_2 dq_1 dq_2}{(2\pi)^4} \phi(p_1) \phi(p_2) \phi(q_1) \phi(q_2) 2\pi \delta(p_1 + p_2 - q_1 - q_2) \\ \times \frac{P}{(p_1 - q_1)^2} \cos\left[\frac{1}{2}\{\theta^A(p_1) - \theta^A(q_1)\}\right] \cos\left[\frac{1}{2}\{\theta^A(p_2) - \theta^A(q_2)\}\right] \\ = \frac{g^2}{2} \int dx dy [|\bar{\varphi}_c(x)|^2 + |\bar{\varphi}_s(x)|^2] |x - y| [|\bar{\varphi}_c(y)|^2 + |\bar{\varphi}_s(y)|^2], \quad (3.1.34)$$

where we have used the definitions (3.1.30) and (3.1.31). Therefore

$$V_{qq}(0) > 0. \quad (3.1.35)$$

The asymptotic feature or the range of the potentials are determined by the overlap of the ground state wave function,  $\varphi$ . We can see analytically the qualitative feature of the potentials from the knowledge of the short range and the asymptotic behavior. The signs of the potentials are justified by the following rough estimate. The potential  $V_{qQ}(X)$  originates from  $V_{11} + V_{12} + V_{21} + V_{22}$ .  $V_{11} \sim |x_1 - X/2| \lambda_1^a \lambda_1^a$  and others are similar to the above. Taking the color matrix element (result to  $\lambda_{ij}^a \lambda_{ji}^a$ ) and multiplying the sign  $-1$  which comes from the exchange of the quarks, we know the sign of the  $V_{qQ}(X)$ . The potential  $V_{qq}(X)$  originates from  $V_{12}$ .  $V_{12} \sim -|x_1 - x_2| \lambda_1^a \lambda_2^a$ . Taking the color matrix element and multiplying the sign coming from the quark exchange, the sign of the potential is positive. Similarly, taking the color matrix element to  $V_{12} = -|X| \lambda_1^a \lambda_2^a$  and multiplying the sign  $-1$ , the sign of the potential,  $V_{qQ}(X)$ , is positive.

We present the results of the explicit calculation for potentials due to the quark exchange for two cases  $\xi = 0.5m_A^2$  and  $\xi = 5m_A^2$  which are shown in Figs. 8. The potential,  $V_{qq}$ , is repulsive and the potential,  $V_{qQ}$ , is attractive. The potential,  $V_{QQ}$ , is



positive definite, being attractive at short distance and repulsive in the relatively long distance region while the standard of the distance being given by the size of the heavy meson. The total potential from the quark exchange,  $V_{qq} + V_{qQ} + V_{QQ}$ , is attractive at short distance and repulsive in the relatively long distance. This feature of the potential remains the same for different  $\xi$ 's, and is qualitatively similar to what was observed in the calculation of meson-meson interactions based on the quark model in four dimensions [22].

The range of the potential is determined by the overlap of the wave function,  $\varphi$ . As  $\xi$  increases, the meson wave function gets more localized and therefore the potential becomes shorter ranged. The potential strength increases as  $\xi$  increases, since the basic interactions are proportional to  $\xi$ .

### 3.2 Meson Exchange Potential

Finally we discuss the meson exchange potential. As we will see, the coupling vertex of the heavy meson emitting or absorbing a light meson is of the order of  $1/\sqrt{N}$  and therefore we can restrict ourselves to the one light meson exchange contribution. In the large  $N$  limit, the leading-order diagrams contributing to the meson exchange potential are illustrated in Figs. 9. To leading order in  $1/N$ , one of the above vertex corresponding to Fig. 10(a) is

$$\Gamma_{3M}^{1n}(p) = \frac{1}{\sqrt{N}} \frac{N}{2} \int \frac{dq_2}{2\pi} \phi(q_2) \times \int \frac{d^2k}{(2\pi)^2} \bar{u}^A(q_2) i g \gamma^0(-i) \frac{P}{(q_2 - k)^2} \Psi^n(p^\mu, k^\mu) i g \gamma^0 u^A(q_2 - p) \phi(q_2 - p), \quad (3.2.1)$$

where the factor  $\frac{1}{\sqrt{N}} \frac{N}{2}$  is the result of  $\frac{1}{\sqrt{N}} \frac{\lambda_2^*}{2} \frac{1}{\sqrt{N}} \frac{\lambda_1^*}{2} \frac{1}{\sqrt{N}}$  and  $n$  is the quantum number of a light meson state, the light meson consisting of a light quark and a light antiquark, i.e. their flavors being  $A$ . Using Eqs. (2.1.32) and (2.1.14), we have

$$\Gamma_{3M}^{1n}(p) = \frac{1}{\sqrt{N}} \frac{i\xi}{2\pi} \int dq_2 \phi(q_2) \phi(q_2 - p) \times P \int \frac{dk}{(q_2 - k)^2} u^{A\dagger}(q_2) \phi^n(p, k) \gamma^0 u^A(q_2 - p). \quad (3.2.2)$$

Neglecting  $\phi_-^n$ 's which corresponds to dropping the contributions from backward-moving string structure (the justification of which was given in Sec. 2.2), we find

$$\Gamma_{3M}^{1n}(p) = \frac{1}{\sqrt{N}} \frac{-i\xi}{2\pi} \int dq_2 \phi(q_2) \phi(q_2 - p) \times P \int \frac{dk}{(q_2 - k)^2} \phi_+^n(p, k) \sin\left[\frac{1}{2}\{\theta^A(p - k) + \theta^A(q_2 - p)\}\right] \times \cos\left[\frac{1}{2}\{\theta^A(k) - \theta^A(q_2)\}\right], \quad (3.2.3)$$

where we used Eqs. (2.1.18), (2.1.20), (2.1.35), (2.1.36) and (2.1.37). The other vertex of the heavy meson absorbing a light meson shown in Fig. 10(b) is given by



$$\Gamma_{3M}^{2n}(p) = \frac{1}{\sqrt{N}} \frac{N}{2} \int \frac{dq_2}{2\pi} \phi(q_2) \phi_+^n(p, q_2) \times \int \frac{d^2 q_1}{(2\pi)^2} \bar{v}^A(p - q_2) i g \gamma^0(-i) \frac{P}{(q_2 - p - q_1)^2} \Psi_H(q_1^\mu)(-i) g \gamma^0 v^B, \quad (3.2.4)$$

where

$$\Psi_H(p^\mu) = \lim_{m_B \rightarrow \infty} \Psi(r^\mu, p^\mu). \quad (3.2.5)$$

Write

$$\phi_H(p) = \int \frac{dp^0}{2\pi} \Psi_H(p^\mu), \quad (3.2.6)$$

then

$$\Gamma_{3M}^{2n}(p) = \frac{1}{\sqrt{N}} \frac{-i\xi}{2\pi} \int dq_2 \phi(q_2) \phi_+^n(p, q_2) P \int \frac{dq_1}{(q_2 - p - q_1)^2} v^{A^\dagger}(p - q_2) \phi_H(q_1) \gamma^0 v^B. \quad (3.2.7)$$

In the limit of  $m_B \rightarrow \infty$ ,  $\theta^B = 0$  and  $T^B = 1$ . From Eq. (2.1.35), we have

$$\bar{\phi}_H(p) = T^{A^\dagger}(p) \phi_H(p). \quad (3.2.8)$$

And from Eqs. (2.1.36), (2.2.1) and (2.2.2), we get

$$\bar{\phi}_H(p) = \phi(p) M^+. \quad (3.2.9)$$

Substituting Eqs. (3.2.8) and (3.2.9) into Eq. (3.2.7), we find

$$\Gamma_{3M}^{2n}(p) = \frac{1}{\sqrt{N}} \frac{i\xi}{2\pi} \int dq_2 \phi(q_2) \phi_+^n(p, q_2) \times P \int \frac{dq_1}{(q_2 - p - q_1)^2} \phi(q_1) \sin\left[\frac{1}{2}\{\theta^A(q_1) - \theta^A(q_2 - p)\}\right]. \quad (3.2.10)$$

We finally reach the meson exchange potential,  $V_M(X) = \sum_n V_M^n(X)$ , depicted in Figs. 9(a)-(d).

$$iV_M(X) = \sum_{n=1}^{\infty} \int \frac{dp}{2\pi} e^{ipX} \frac{-2i}{\sqrt{p^2 + m_n^2}} [|\Gamma_{3M}^{1n}(p)|^2 + |\Gamma_{3M}^{2n}(p)|^2 + \Gamma_{3M}^{1n}(p) \Gamma_{3M}^{2n*}(p) + \Gamma_{3M}^{2n}(p) \Gamma_{3M}^{1n*}(p)], \quad (3.2.11)$$

where the normalization of the meson wave function is

$$\int \frac{dk}{2\pi} \text{Tr} \phi^\dagger(p, k) \phi(p, k) = 1. \quad (3.2.12)$$

The first, second, third and fourth terms in Eq. (3.2.11) corresponds to Figs. 9(a), (b), (c) and (d), respectively.

We note that the vertices given by Eqs. (3.2.3) and (3.2.10), in the case that the momentum of the exchanged light meson is zero, have the remarkable properties that  $\Gamma_{3M}^{1n}(0) = \Gamma_{3M}^{2n}(0) = 0$  for odd  $n$  and finite for even  $n$  because the integrands except for the light meson wave function are odd functions of  $k$  or  $q_2$ . We see from Eq. (3.2.11) that  $V_M(0) < 0$ . We also find that the spatial integral of  $V_M(X)$  is negative, i.e.

$$\int dX V_M(X) = - \sum_{n=1}^{\infty} \frac{2}{m_n} |\Gamma_{3M}^{1n}(0) + \Gamma_{3M}^{2n}(0)|^2 < 0. \quad (3.2.13)$$

The calculated meson exchange potential is shown in Figs. 11 and 12. To get the meson exchange potential we have to sum over the contributions from the ground and excited states of the light meson which is exchanged between the heavy mesons. We find, in Figs. 11(a) and (b), that the main contributions come from the ground state and the first excited state. The ground state contribution has the feature that the potential is attractive at short distance and is repulsive in the relatively long distance region. Its spatial integral being zero since  $\Gamma_{3M}^{11}(0) = \Gamma_{3M}^{21}(0) = 0$ . The ground state meson has negative parity and corresponds to either a pseudoscalar meson or a vector meson in four dimensions. Our heavy meson also corresponds to either a pseudoscalar meson or a vector meson. There is no spin in two dimensions. In comparing the interactions in two and four dimensions, we take the average over all possible spin states in the latter which is equivalent to considering only the spin-independent central part. The pseudoscalar meson exchange gives only a spin-dependent interaction while the vector



meson exchange interaction contains a central term as its important part. The obtained feature of the potential due to the exchange of the ground state meson is similar to that of the vector meson exchange potential when the vector meson is a composite particle [19]. The first excited state contribution to the potential is attractive. The first excited state corresponds to either a scalar meson or an axial vector meson and the scalar meson exchange gives the central term. The attractive nature is common for two- and four-dimensional world. The total contribution, depicted in Figs. 12, has the feature that the potential is attractive at short distance and is repulsive in the relatively long distance region. The above feature of the potential is not altered by changing the coupling strength  $\xi$ . The meson exchange potential becomes stronger and of shorter ranged as  $\xi$  increases since both the light-meson-heavy-meson coupling and the light meson masses increase with  $\xi$ .

The quark exchange potential, the meson exchange potential and the sum of the two are shown in the same scale in Figs. 13. We find the quark exchange potentials are fairly larger than the meson exchange potentials in both of the two cases  $\xi = 0.5m_A^2$  and  $\xi = 5m_A^2$ , though the relative importance of the meson exchange contribution increases as the ratio  $\xi/m_A^2$  becomes larger. The meson exchange potential has a longer range with exponential tail while the quark exchange potential decreases more rapidly as  $X$  increases.

## 4 Summary and Conclusion

We have studied in this thesis some of the features of hadron spectra and hadron-hadron interactions in  $QCD_2$  for the purpose of obtaining insights to similar problems in the real world. More specifically we have discussed here the interaction between two heavy mesons each consisting of a light quark and a heavy antiquark in large  $N$  limit.

For this purpose, we have first solved the meson problem which is explicitly solvable in  $QCD_2$  in the large  $N$  limit. There have been two ways to construct the meson states, i.e. the 't Hooft method in the light-cone formulation and that of Bars and Green in the ordinary coordinate formulation. Bars and Green have proved the equivalence of the two for the finite constituent quark mass. In the case where one of the quark masses is infinitely heavy, however, the equivalence has not been established. We have therefore examined the equivalence numerically for the infinite antiquark mass limit and established the equivalence. It implies that the gauge invariance of the meson spectrum also holds for the heavy mesons. For the light meson, we calculated the energy spectra,  $r_n^0$ , for finite momentum,  $r$ , and saw the relation,  $(r_n^0)^2 - r^2 = m_n^2$ , indicating the Lorentz invariance of the meson spectra.

Using the heavy meson wave function obtained in the ordinary coordinate, we turned to the problem of the interaction. The light antiquarks do not appear in the heavy meson wave function to the lowest order in  $1/N$ . We considered the interactions which take into account the role of light antiquarks separately from the residual interactions. The only role of the light antiquarks is to give rise to the light meson exchange potential. The remaining interactions are caused by the exchange of light quarks within the framework of the ordinary quantum mechanics. This can therefore be considered



as an actual example of the hybrid model for hadron-hadron interactions [18,19] where the quark exchange and the meson exchange contributions are unified in a natural way. (The hybrid model in which the quark exchange and the meson exchange are combined to explain the hadron-hadron interaction has been partially successful in describing hadronic interactions in the real world of four dimensions but its theoretical basis has not been established so far.)

In the quark exchange potentials we showed that there are three types of interactions which are the contribution from the Coulomb potential between light quarks,  $V_{qq}$ , that between light quark and heavy antiquark,  $V_{qQ}$ , and that between heavy antiquarks,  $V_{QQ}$ . We presented the results of the explicit calculation for potentials due to the quark exchange as a function of the spatial separation between the two heavy mesons for two cases  $\xi = 0.5m_A^2$  and  $\xi = 5m_A^2$ . The potential,  $V_{QQ}$ , is found to be positive definite, being attractive at short distance and repulsive in the relatively long distance region, the potential,  $V_{qQ}$ , is attractive and the potential,  $V_{qq}$ , is repulsive. We showed that the qualitative features of  $V_{QQ}$ ,  $V_{qQ}$  and  $V_{qq}$  can be understood without numerical calculations by studying their short range parts and their asymptotic behaviors. The total potential,  $V_{qq} + V_{qQ} + V_{QQ}$ , is attractive at short distance and repulsive in the relatively long distance region. This is similar to what has been observed in the quark cluster model calculations of meson-meson interaction in four dimensions [22]. It seems that once we accept the potential picture, the basic features of the hadron-hadron interactions do not depend on the dimensionality.

To get the meson exchange potential we have summed over the contributions from the ground and excited states of the light meson which is exchanged between the heavy mesons. The rough estimate for each contributions,  $V_M^n(X)$ , are available analytically.

The short distance behavior of these are determined by the inequality  $V_M^n(0) < 0$ . We also observe that  $\int dX V_M^n(X)$  is zero for odd  $n$  and is negative for even  $n$ . We presented the results of the explicit calculation for potentials due to the meson exchange for two cases  $\xi = 0.5m_A^2$  and  $\xi = 5m_A^2$ . Main contributions are from the ground state ( $n = 1$ ) and the first excited state ( $n = 2$ ). The meson exchange potential also has several features similar to those in the real world. The ground state contribution to the potential is attractive at short distance and repulsive in the relatively long distance region as is inferred from the above observation. The ground state light meson exchange corresponds to the exchange of a vector meson in four dimensions and the resulting potential has the same behavior as what one expects from the exchange of a composite vector meson. The first excited state contribution is attractive as is also inferred from the above observation. The exchange of the first excited state meson corresponds to that of a scalar meson in four dimensions and the attractive nature is common for both dimensions. The total potential for the meson exchange is attractive at short distance and repulsive in the relatively long distance region. In two cases, i.e.  $\xi = 0.5m_A^2$  and  $\xi = 5m_A^2$ , the quark exchange potential is dominant in the short and medium range parts while the meson exchange potential has a longer tail. The relative importance of the latter increases as the coupling strength,  $\xi$ , increases.

The present study has thus shown that the hadron physics based on QCD<sub>2</sub> has many aspects in common with the hadron physics in the real world and its close examination will be useful in getting analytical insights of four dimensional QCD.



### Acknowledgement

I wish to express my gratitude to my academic supervisor, Prof. Koichi Yazaki, for a lot of guidance and discussion.

### References

- [1] H. D. Politzer, Phys. Rep. 14C (1974) 129.
- [2] R. P. Feynman, Photon-Hadron Interactions, Benjamin, Reading 1972.
- [3] A. De Rújula, H. Georgi and S. L. Glashow, Phys. Rev. D12 (1975) 147; N. Isgur and G. Karl, Phys. Lett. B72 (1977) 109; Phys. Rev. D19 (1979) 2653; D20 (1979) 1191.
- [4] M. Oka and K. Yazaki, in Quarks and Nuclei, ed. W. Weise (World Scientific, 1984) p. 489; K. Shimizu, Rep. Prog. Phys. 52 (1989) 1.
- [5] I. Bars and M. B. Green, Phys. Rev. D 17 (1978) 537.
- [6] One of the examples which refers to the necessity of the spontaneous chiral symmetry breaking in four dimensional QCD is F. J. Ynduráin, Quantum Chromodynamics (Springer-Verlag, 1983).
- [7] S. Coleman, Commun. Math. Phys. 31 (1973) 259.
- [8] A. R. Zhitnitsky, Phys. Lett. 165B (1985) 405.
- [9] M. Li, Phys. Rev. D 34 (1986) 3888.
- [10] L. L. Salcedo, S. Levit and J. W. Negele, Nucl. Phys. B361 (1991) 585.
- [11] M. Burkardt, Ph. D. Thesis (Erlangen-Nürnberg, 1989).
- [12] G. 't Hooft, Nucl. Phys. B75 (1974) 461.
- [13] M. B. Einhorn, Phys. Rev. D 14 (1976) 3451.



- [14] J. H. Weis, Acta Phys. Pol. B9 (1978) 1051.
- [15] C. G. Callan, Jr., N. Coote and D. J. Gross, Phys. Rev. D 13 (1976) 1649.
- [16] R. C. Brower, J. Ellis, M. G. Schmidt and J. H. Weis, Nucl. Phys. B128 (1977) 131; 175.
- [17] J. Ellis, Acta Phys. Pol. B8 (1977) 1019.
- [18] Y. Yamauchi, R. Yamamoto and M. Wakamatsu, Nucl. Phys. A443 (1985) 628.
- [19] K. Yazaki, in Perspectives of Meson Science, eds. T. Yamazaki, K. Nakai and K. Nagamine Ch. 26 (1992) p. 795.
- [20] M. Li, L. Wilets and M. C. Birse, J. Phys. G: Nucl. Phys. 13 (1987) 915.
- [21] E. Witten, Nucl. Phys. B160 (1979) 57; S. Coleman,  $1/N$ , in Aspects of Symmetry (Cambridge Univ. Press, 1985) p. 351.
- [22] F. Lenz, J. T. Londergan, E. J. Moniz, R. Rosenfelder, M. Stingl and K. Yazaki, Ann. Phys. 170 (1986) 65; E. S. Swanson, Ann. Phys. 220 (1992) 73.

Table 1. The heavy meson spectra,  $(r_n^0 - m_B)/m_A$ , in the axial gauge and those,  $(\sqrt{r_n^2} - m_B)/m_A$ , in the light-cone gauge for two different  $\xi$ 's. The values in the first column represent quantum numbers of the meson state.

$n$	$\xi = 0.5m_A^2$		$\xi = 5m_A^2$	
	axial gauge	light-cone gauge	axial gauge	light-cone gauge
1	1.73	1.73	3.54	3.54
2	2.84	2.83	7.47	7.42
3	3.58	3.56	10.1	10.0
4	4.20	4.16	12.2	12.2
5	4.73	4.69	13.9	14.0



Table 2. The light meson spectra,  $r_n^0/m_A(r=0)$ , in the axial gauge and those,  $\sqrt{r_n^2}/m_A$ , in the light-cone gauge for two different  $\xi$ 's. The spectra in the columns named by axial gauge are calculated by Eq. (2.2.3).

$n$	$\xi = 0.5m_A^2$		$\xi = 5m_A^2$	
	axial gauge	light-cone gauge	axial gauge	light-cone gauge
1	2.72	2.70	4.13	3.94
2	4.15	4.15	9.41	9.40
3	5.18	5.19	13.2	13.2
4	6.02	6.06	16.2	16.3
5	6.76	6.81	18.7	18.9

Table 3(a). The light meson energy spectra,  $r_n^0/m_A$ , in the finite momentum calculated by Eq. (2.2.3) in the case  $\xi = 0.5m_A^2$ .

$n$	$r/m_A = 0$	$r/m_A = 2$	$r/m_A = 4$	$r/m_A = 6$	$r/m_A = 8$
1	2.72	3.38	4.82	6.58	8.45
2	4.15	4.60	5.75	7.30	9.02
3	5.18	5.54	6.53	7.93	9.54
4	6.02	6.35	7.22	8.51	10.0



Table 3(b). The light meson energy spectra,  $r_n^0/m_A$ , in the finite momentum calculated by Eq. (2.2.3) in the case  $\xi = 5m_A^2$ .

$n$	$r/m_A = 0$	$r/m_A = 2$	$r/m_A = 4$	$r/m_A = 6$	$r/m_A = 8$
1	4.13	4.67	5.58	7.19	8.92
2	9.41	9.71	10.1	11.1	12.3
3	13.2	13.4	13.6	14.4	15.3
4	16.2	16.4	16.5	17.2	18.0

## Figure Captions

Fig. 1.  $\theta(p)$  for two cases (a)  $\xi = 0.5m_A^2$  and (b)  $\xi = 5m_A^2$ .

Fig. 2. The quark single particle energy as a function of  $p$ . (a)  $\xi = 0.5m_A^2$ , (b)  $\xi = 5m_A^2$ .

Fig. 3. The next order contributions going beyond the Hartree-Fock approximation in perturbation theory to the total energy.

Fig. 4. Diagrammatic representation of Eq. (2.1.31).

Fig. 5. (a)  $C(p, k, r)$ , (b)  $-S(p, k, r)$ , (c) an example of the graph constructing a meson.

Fig. 6. The heavy meson ground state wave function,  $\varphi(x)$ , for two cases (a)  $\xi = 0.5m_A^2$  and (b)  $\xi = 5m_A^2$ .

Fig. 7. Diagrammatic representations for the quark exchange potentials: The contributions from (a) the Coulomb potential between a light quark and a heavy antiquark, (b) that between light quarks and (c) that between heavy antiquarks.

Fig. 8. The quark exchange potentials as a function of the distance between the heavy mesons for two different cases (a)  $\xi = 0.5m_A^2$  and (b)  $\xi = 5m_A^2$ .

Fig. 9. Diagrammatic representations for the meson exchange potential.

Fig. 10. The three meson vertices contribute to the meson exchange potential.

Fig. 11. The meson exchange potentials as a function of the distance between the heavy mesons. The contributions from the several states of the light meson are shown for two different cases (a)  $\xi = 0.5m_A^2$  and (b)  $\xi = 5m_A^2$ .  $n$  is a quantum number of the light meson.



Fig. 12. The total meson exchange potential. (a)  $\xi = 0.5m_A^2$ , (b)  $\xi = 5m_A^2$ .

Fig. 13. The quark exchange potential, the meson exchange potential and the sum of two. (a)  $\xi = 0.5m_A^2$ , (b)  $\xi = 5m_A^2$ .

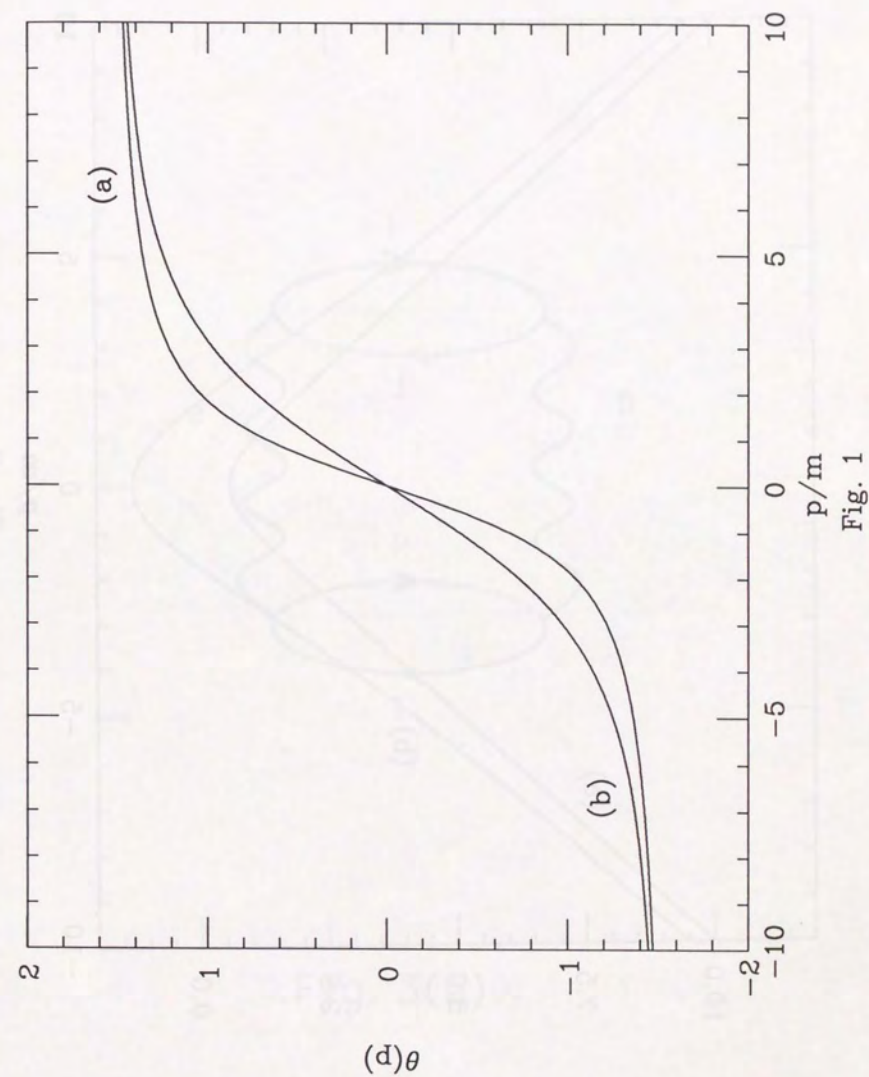


Fig. 1



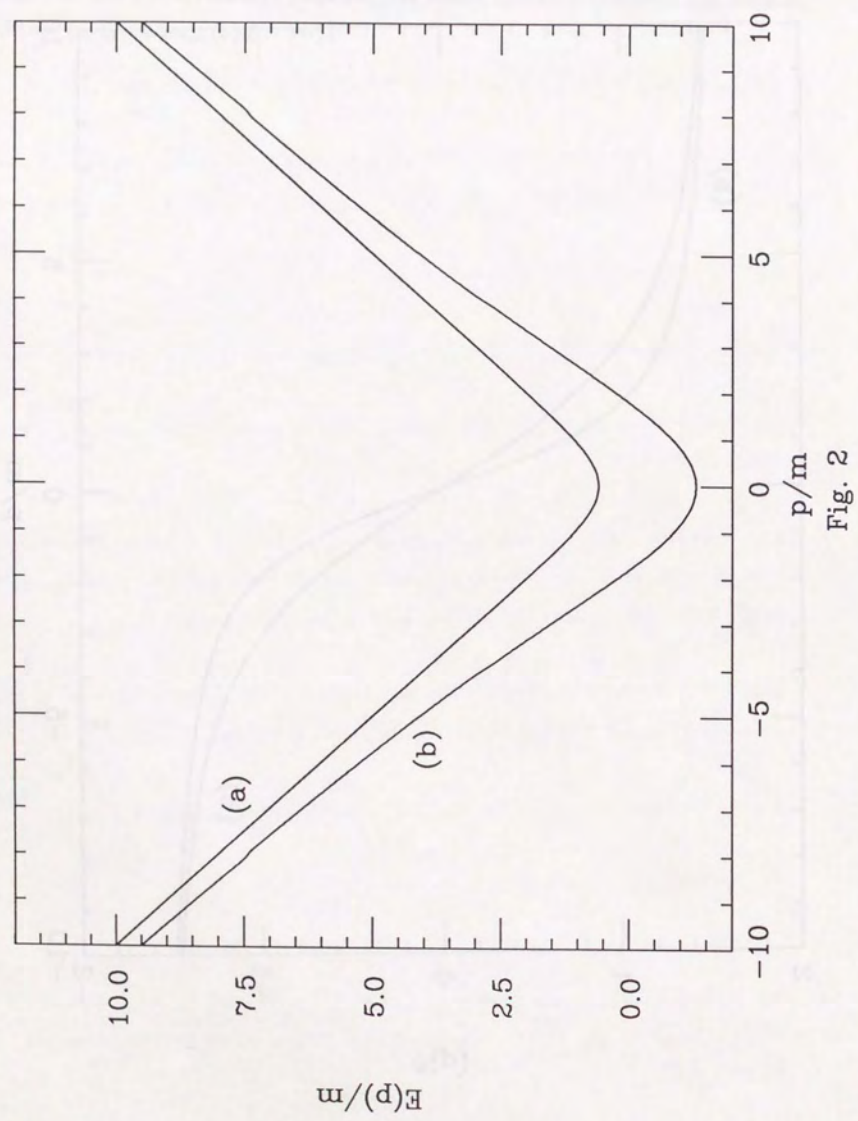


Fig. 2

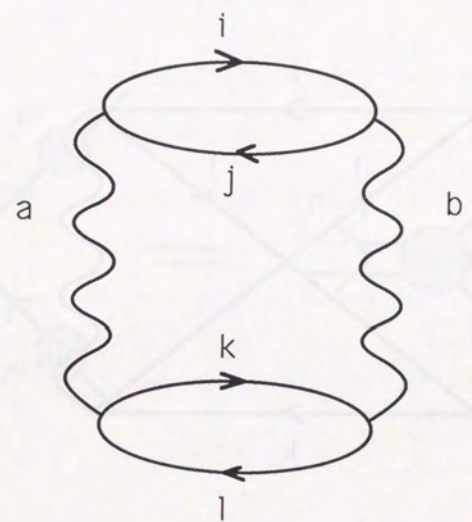


Fig. 3(a)



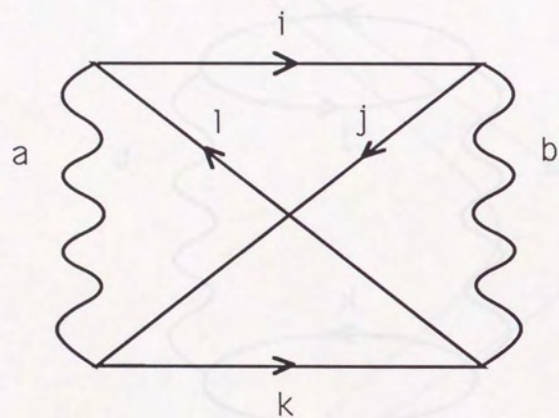


Fig. 3(b)

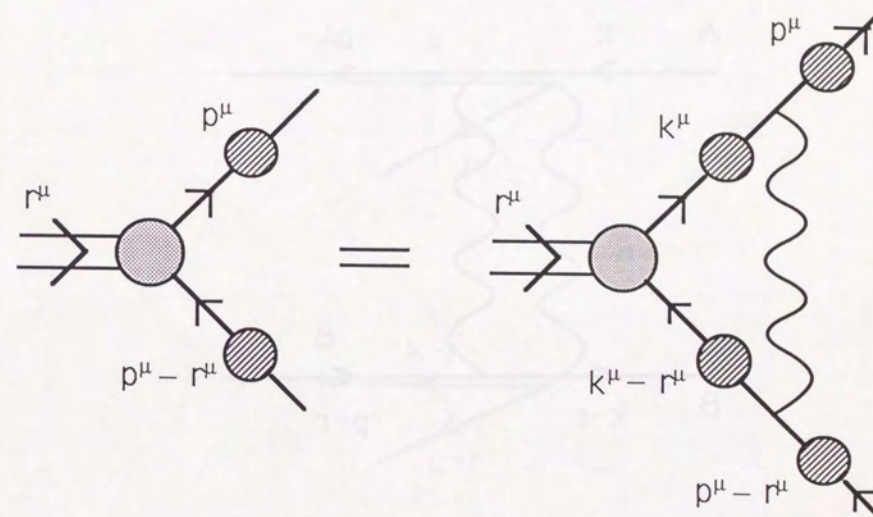


Fig. 4



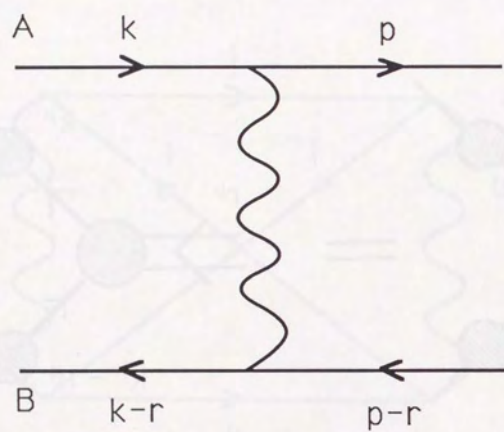


Fig. 5(a)

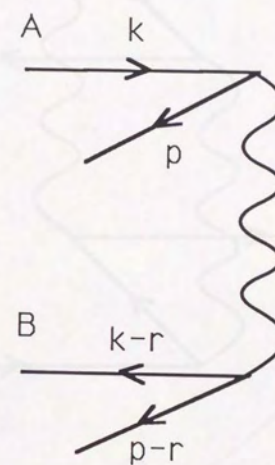


Fig. 5(b)



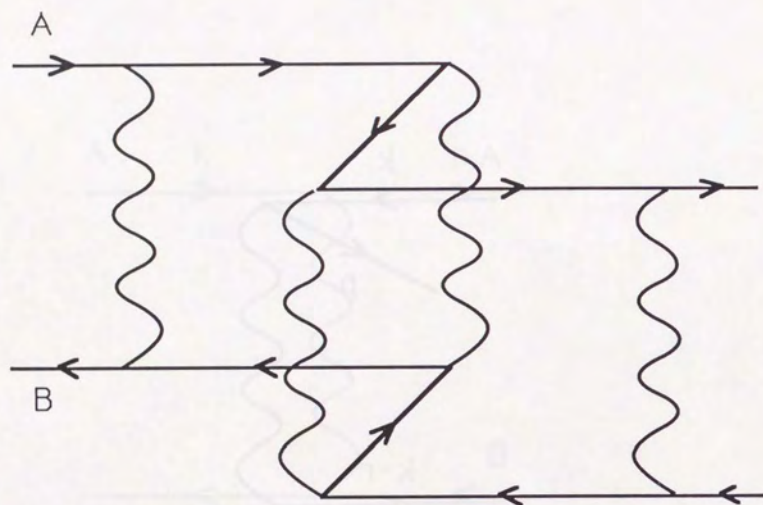


Fig. 5(c)

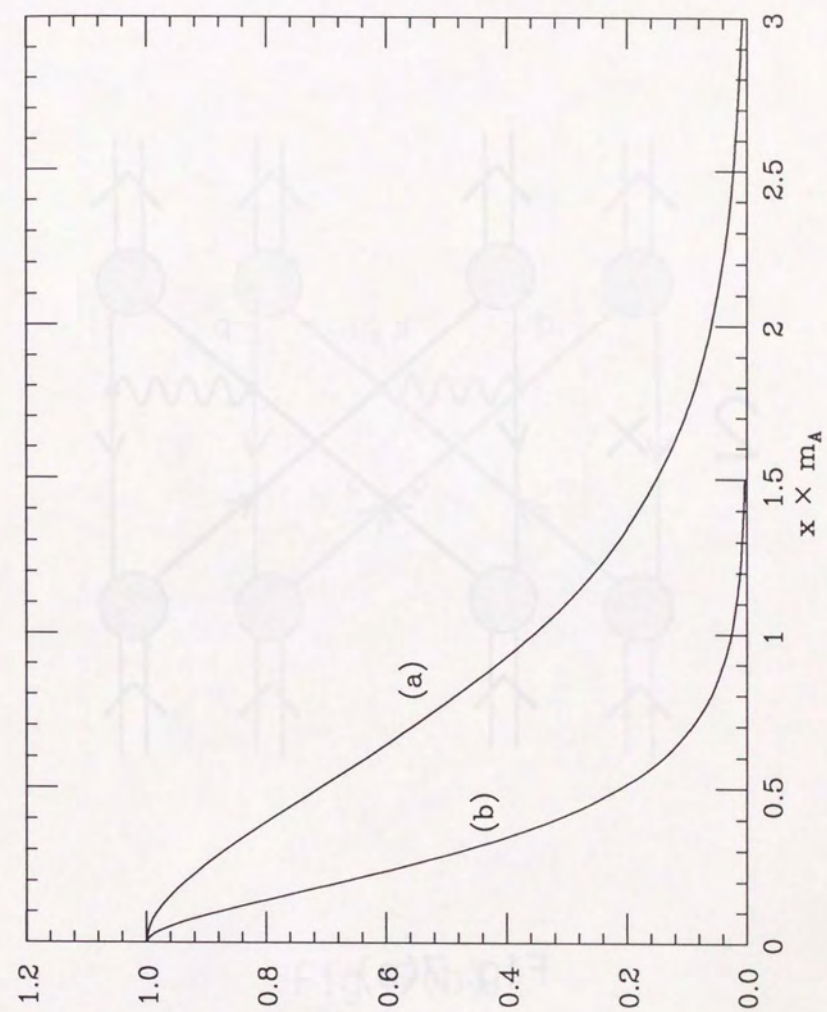


Fig. 6



2 ×

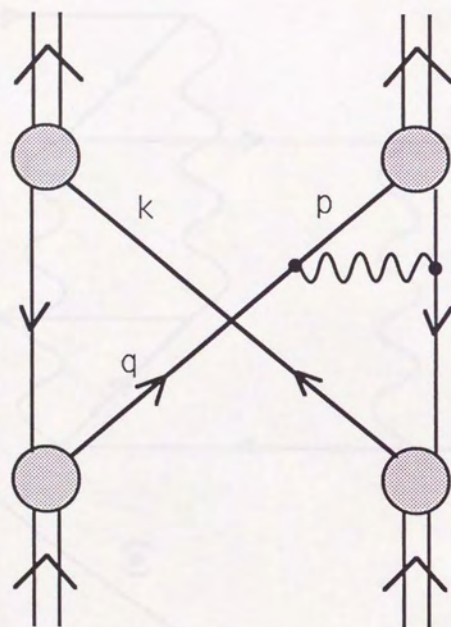


Fig. 7(a)

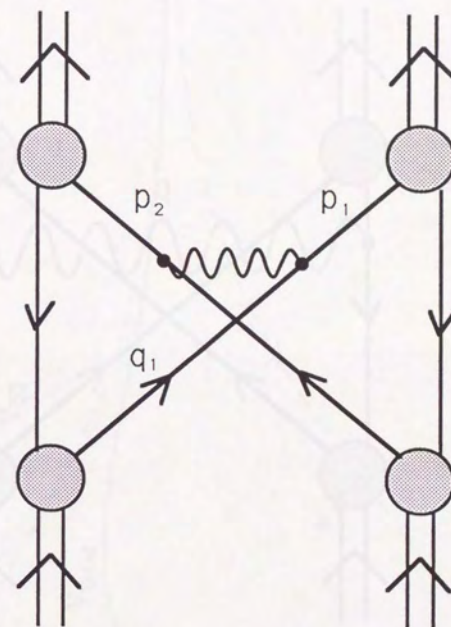


Fig. 7(b)



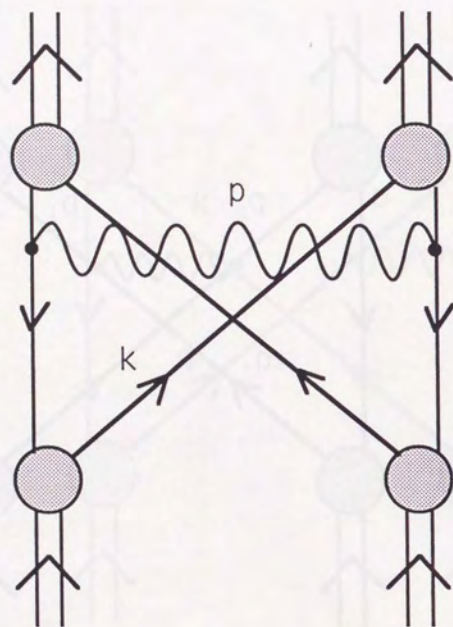


Fig. 7(c)

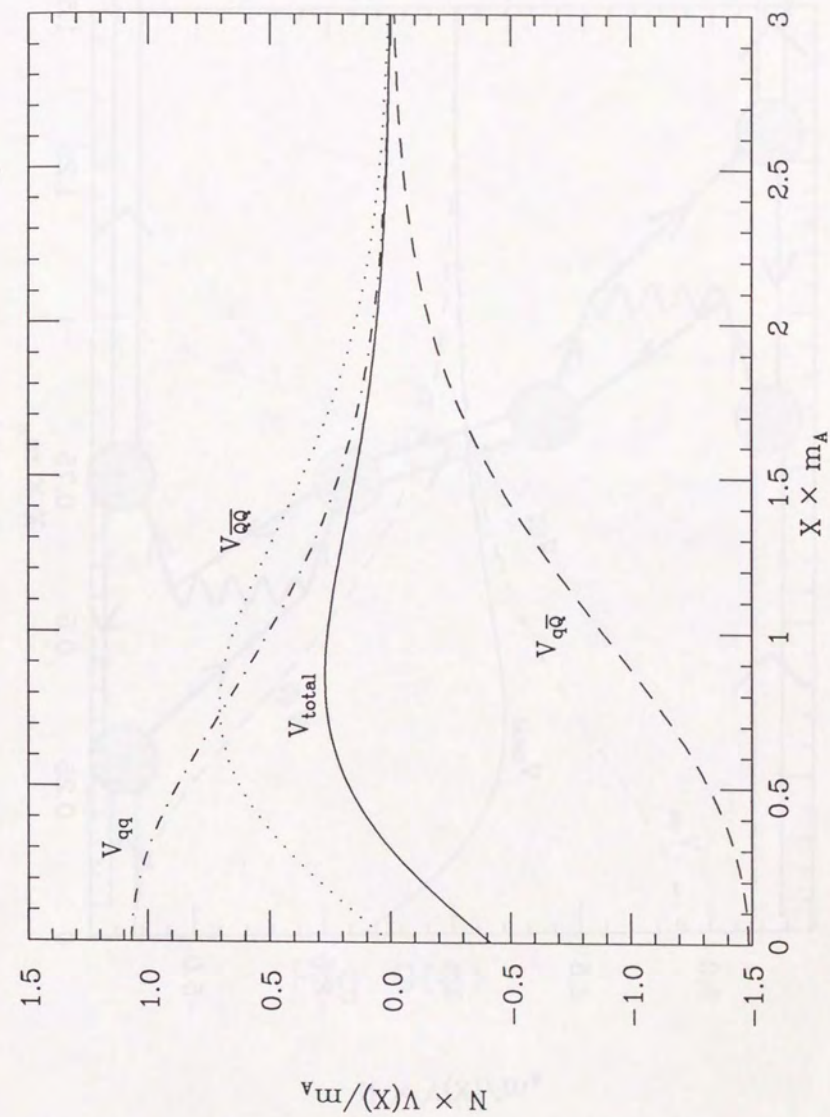


Fig. 8(a)



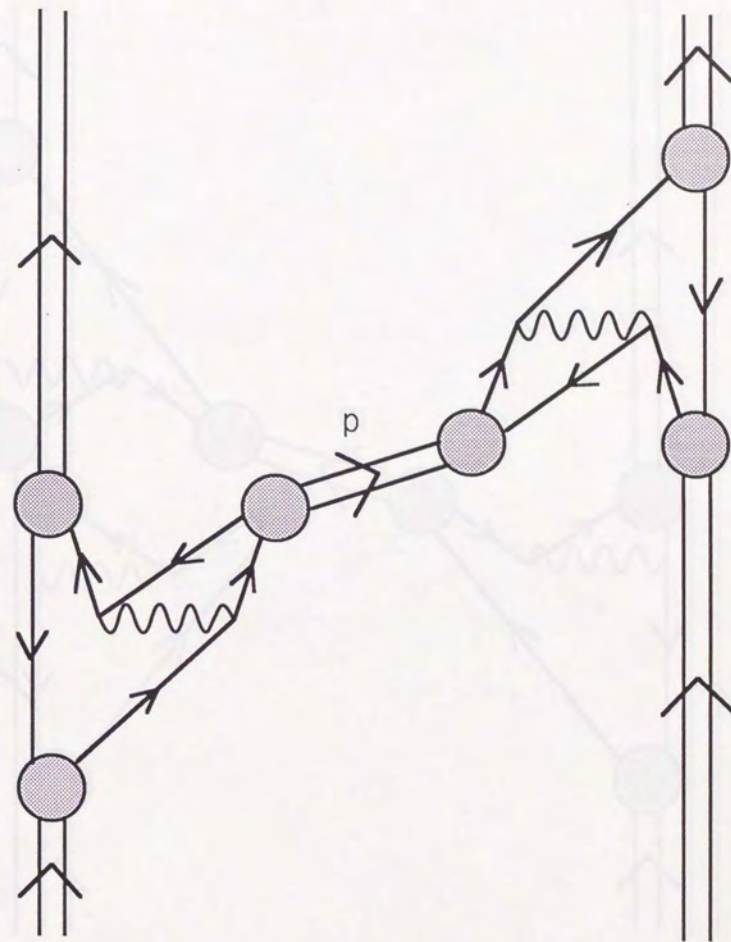
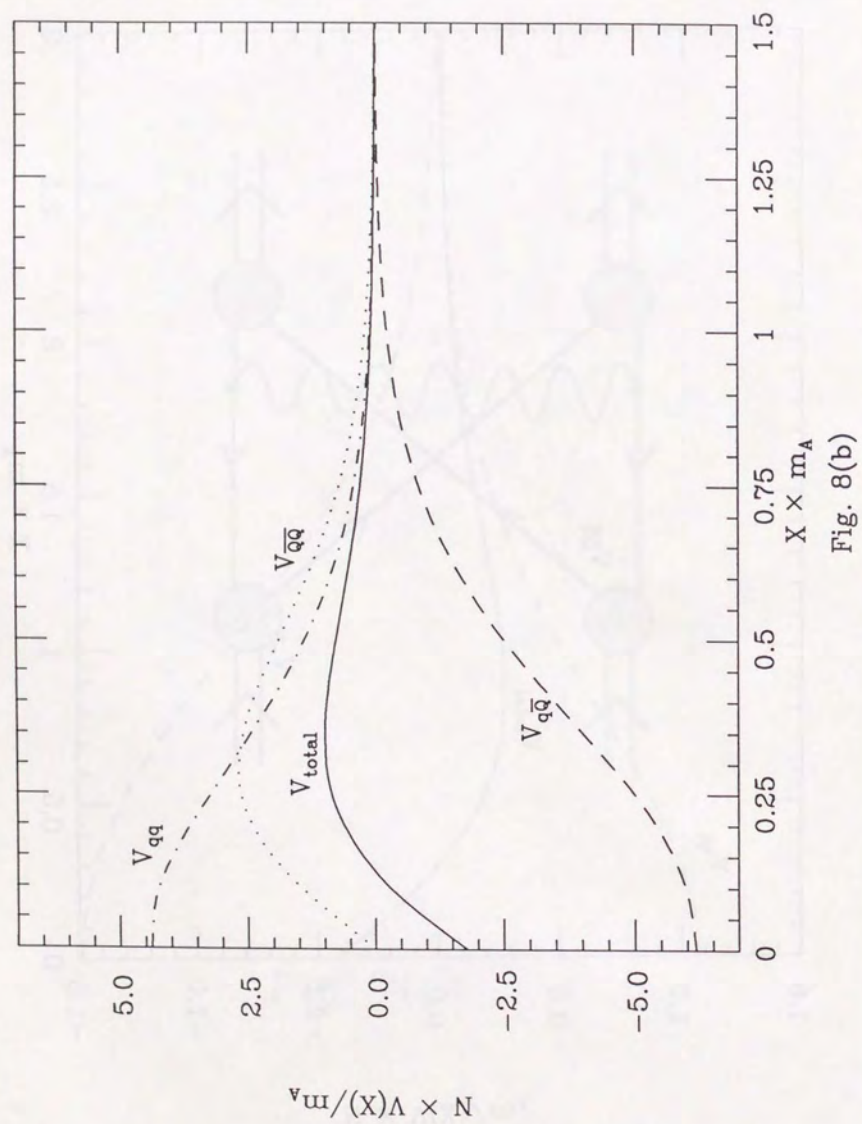


Fig. 9(a)



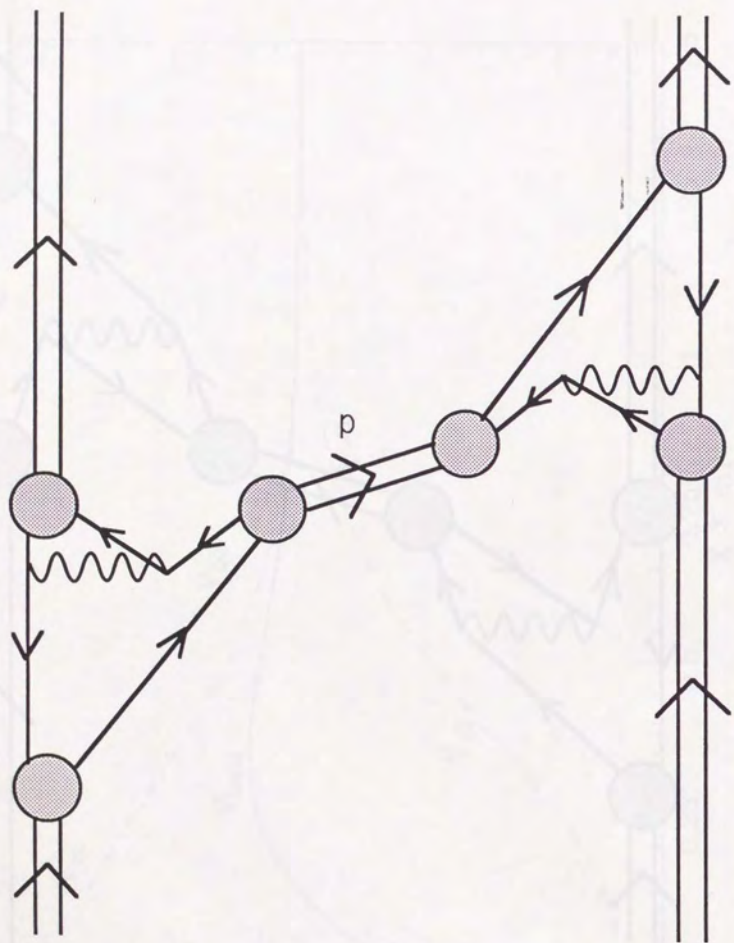


Fig. 9(b)

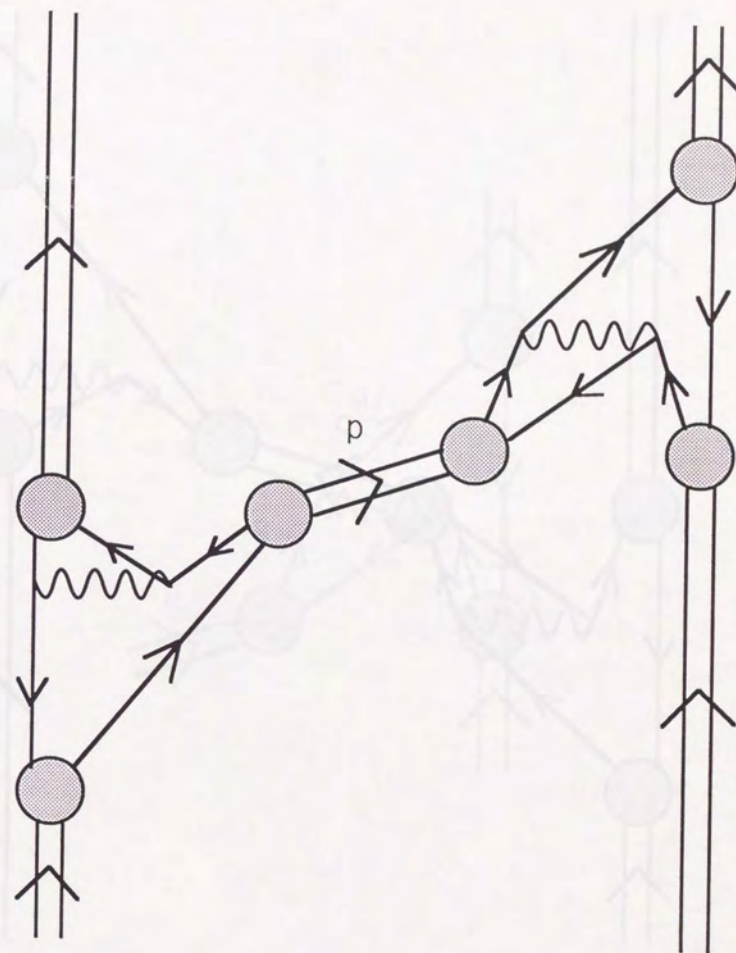


Fig. 9(c)



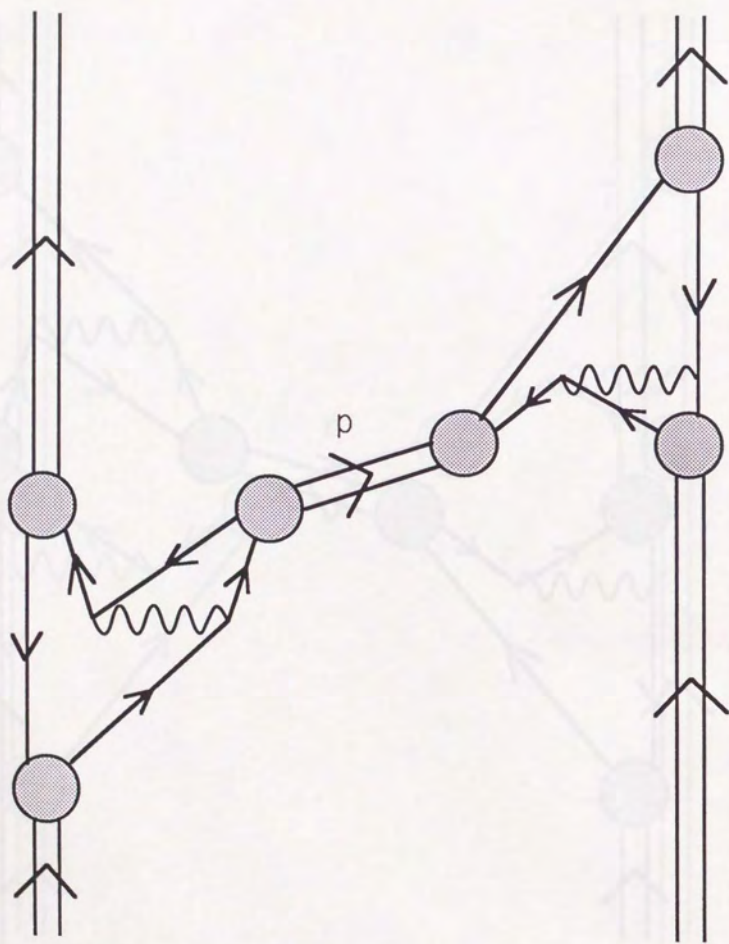


Fig. 9(d)

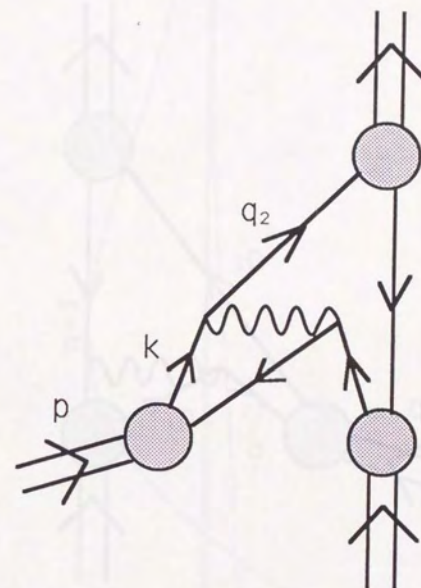


Fig. 10(a)



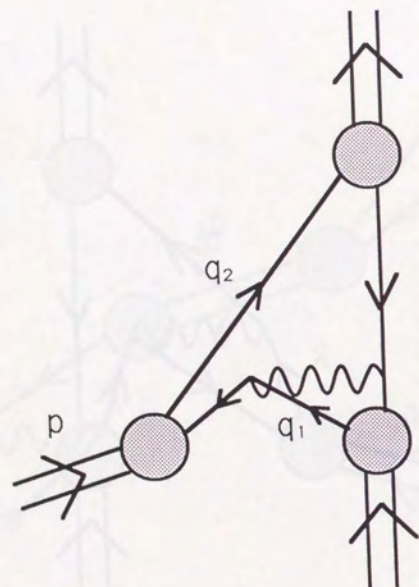


Fig. 10(b)

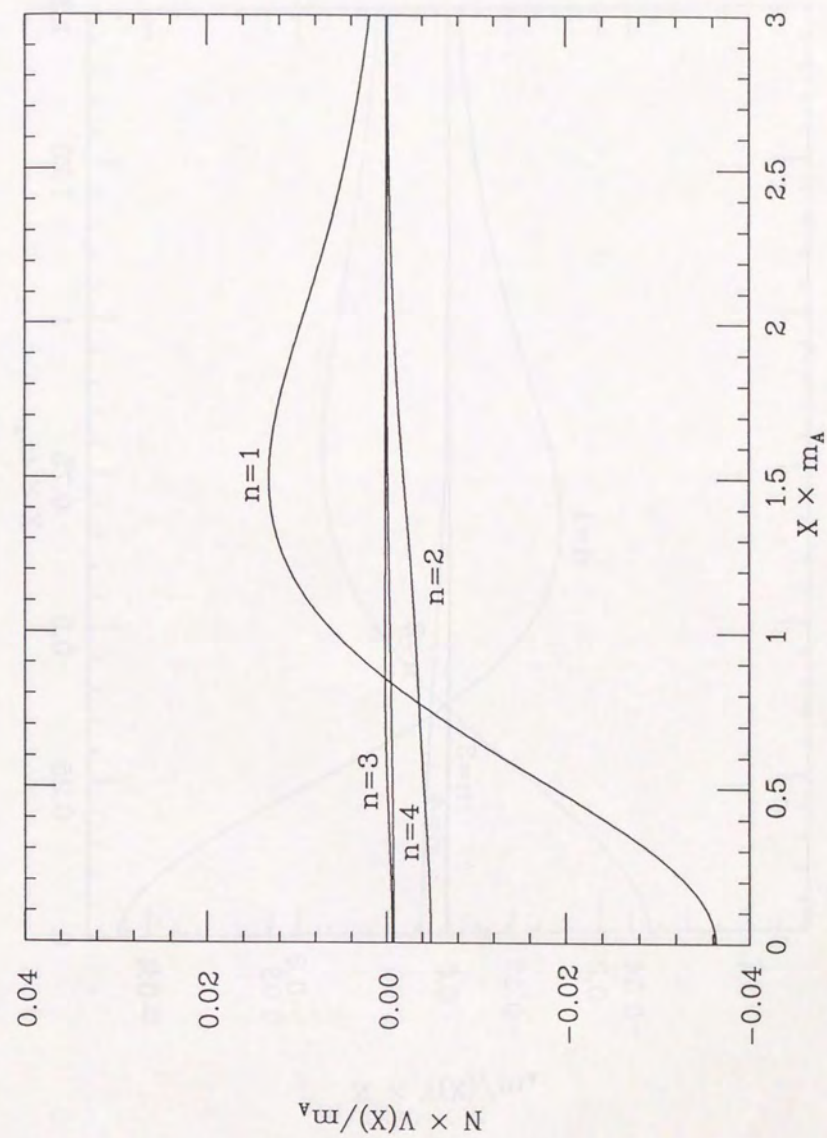


Fig. 11(a)



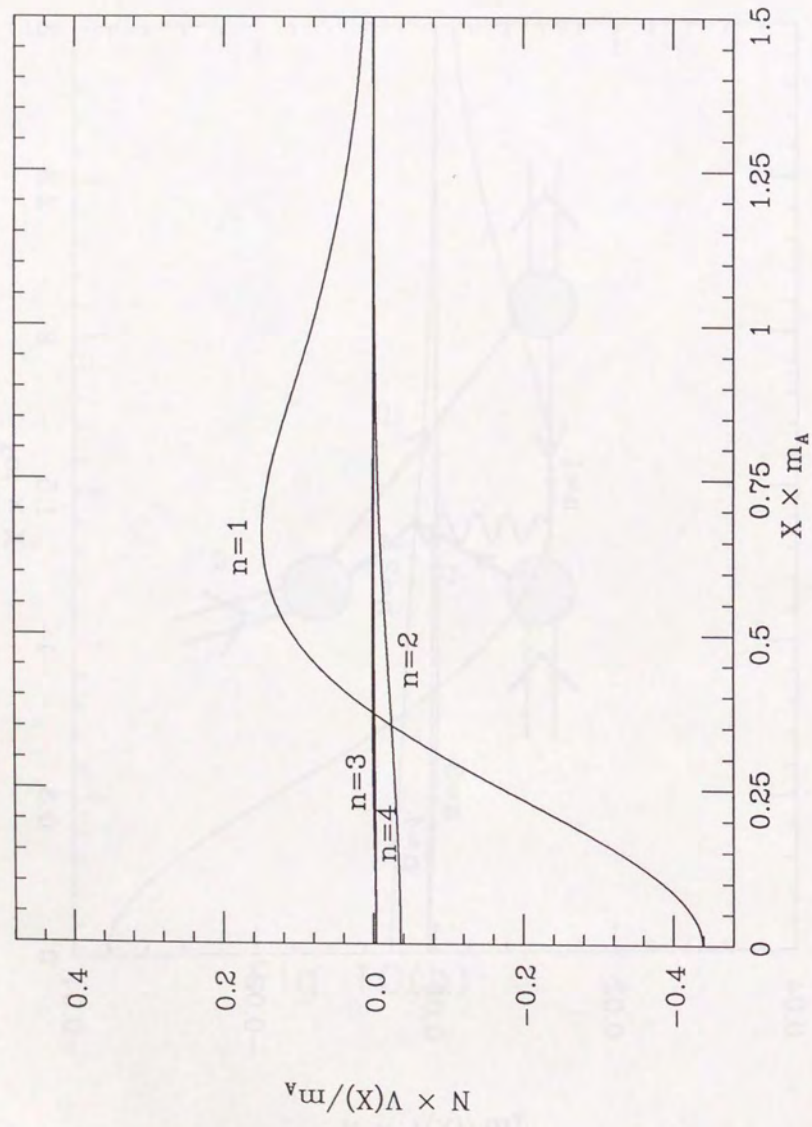


Fig. 11(b)

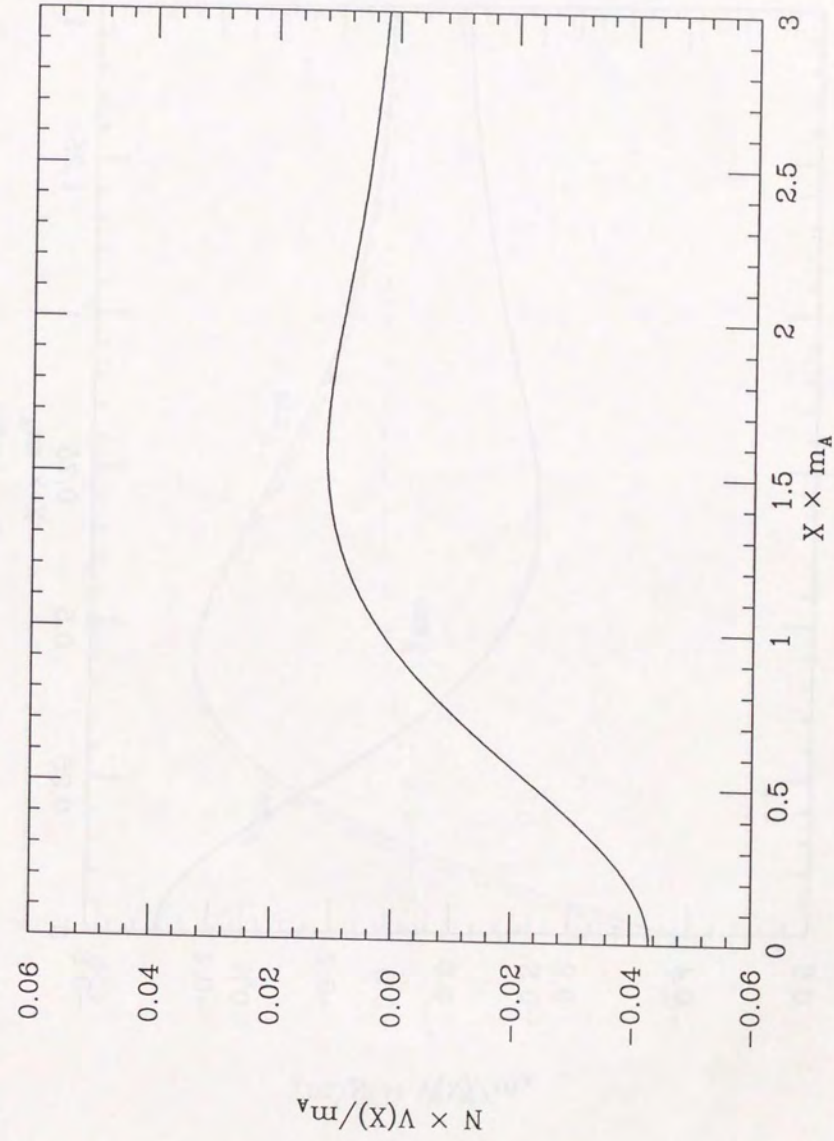


Fig. 12(a)



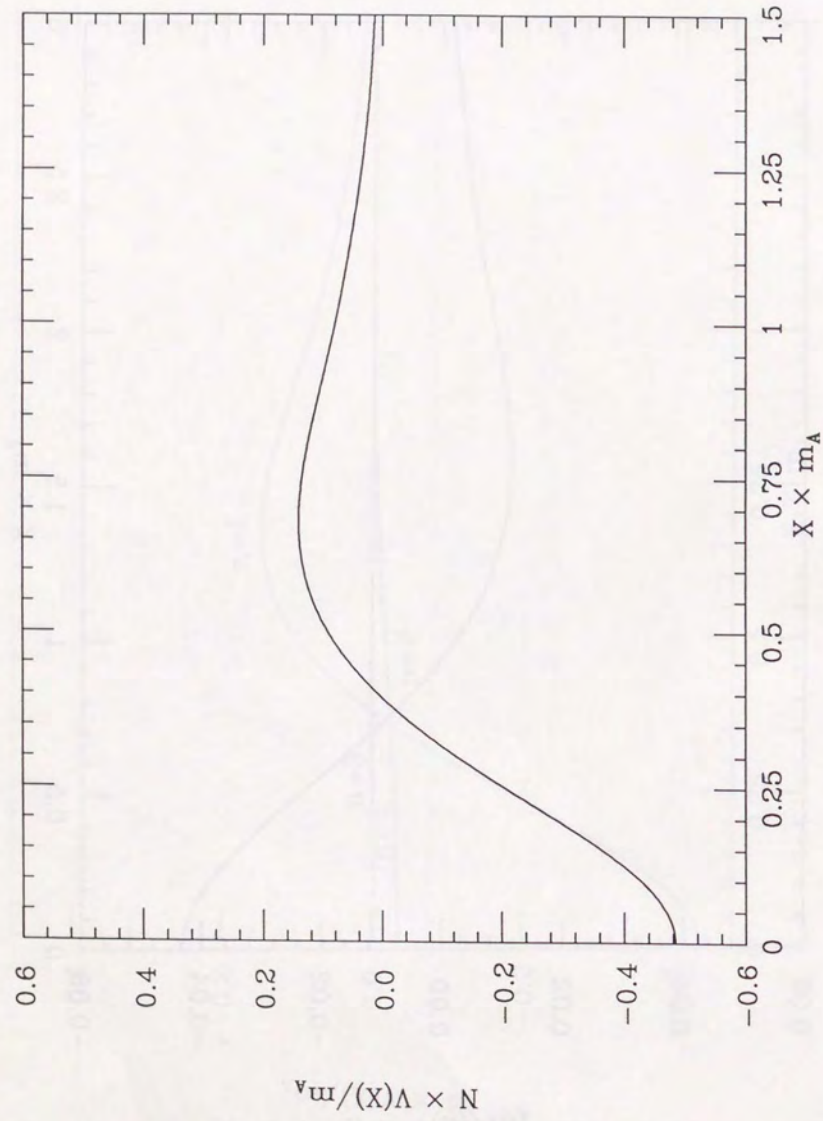


Fig. 12(b)

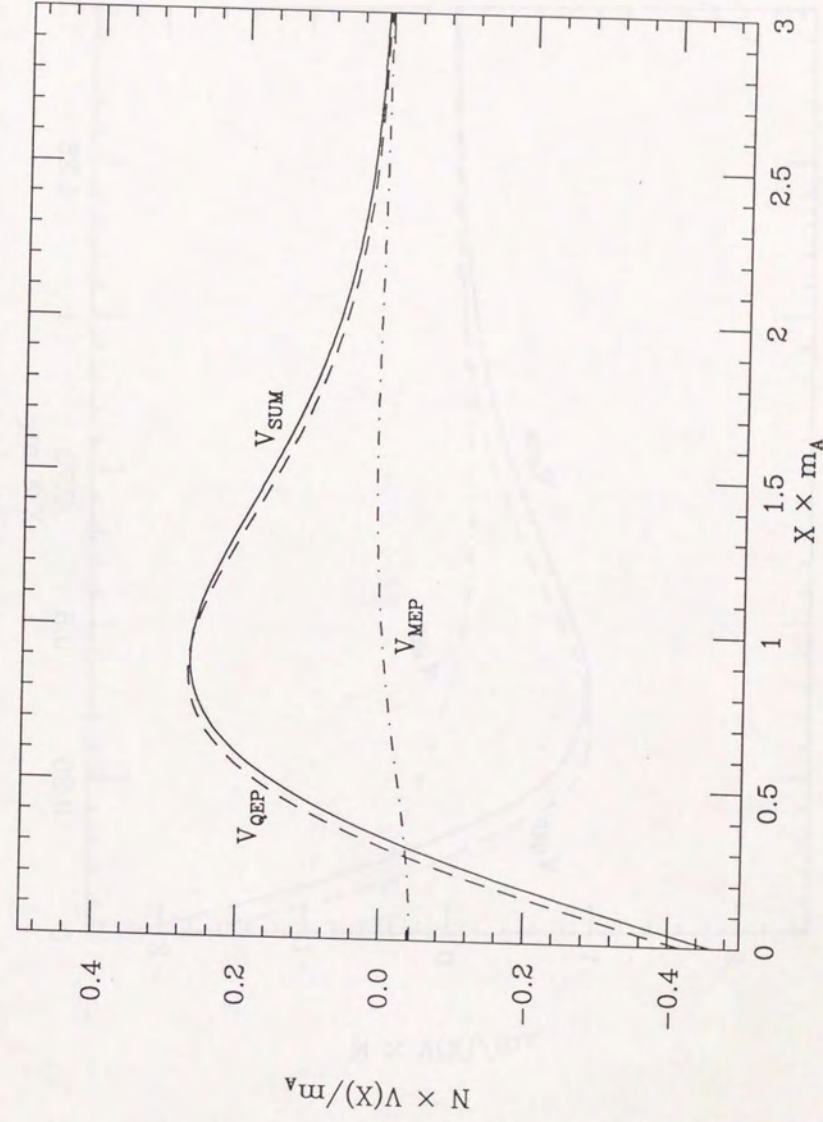


Fig. 13(a)



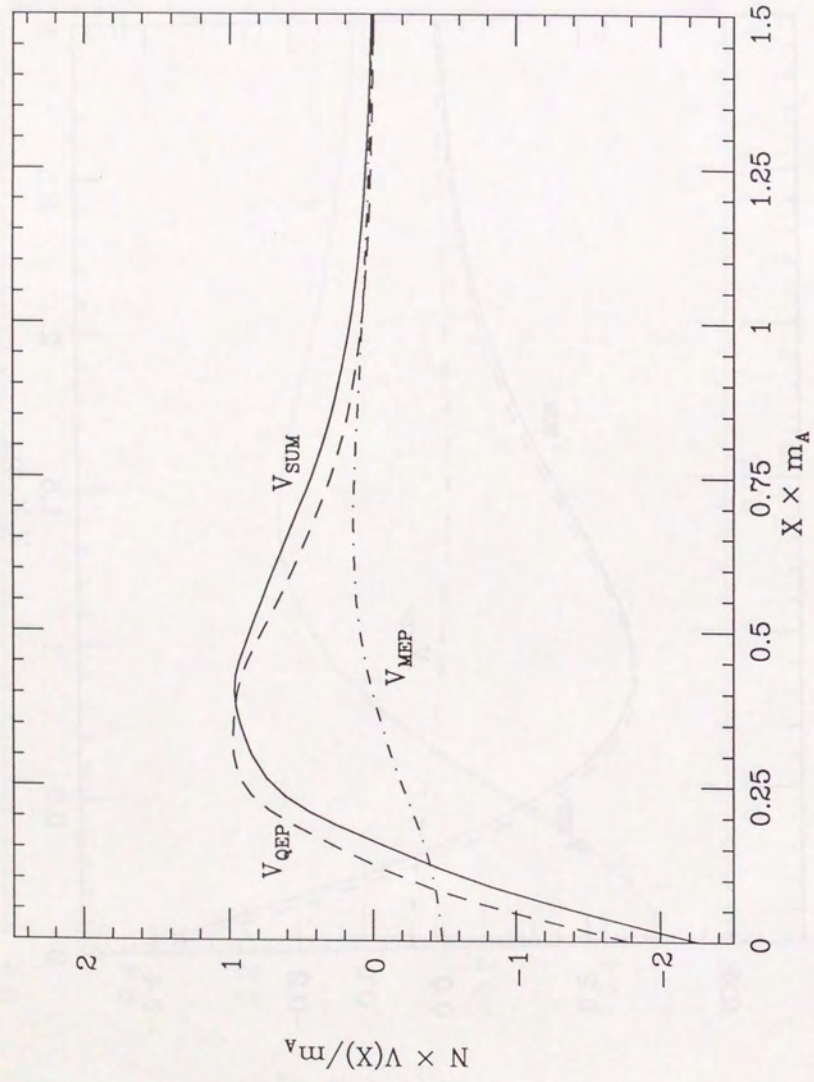


Fig. 13(b)



